

Application of UWB Technology for Positioning , a Feasibility Study

Senad Canovic

Master of Science in Electronics
Submission date: October 2007
Supervisor: Geir Egil Øien, IET

Problem Description

The thesis consists of:

- 1- Study and understating of the UWB technology
- 2- Study and understanding of methods and principals for/behind positioning using the UWB technology.
- 3- Identification of a few suitable methods for practical implementation of such functionality.
- 4- Comparison of these methods and recommendation of one of them as the most suitable implementation method.

Assignment given: 05. February 2007

Supervisor: Geir Egil Øien, IET

Summary

Ultra wideband (UWB) signaling and its usability in positioning schemes has been discussed in this report. A description of UWB technology has been provided with a view on both the advantages and disadvantages involved. The main focus has been on Impulse Radio UWB (IR-UWB) since this is the most common way of emitting UWB signals. IR-UWB operates at a very large bandwidth at a low power. This is based on a technique that consists of emitting very short pulses (in the order of nanoseconds) at a very high rate. The result is low power consumption at the transmitter but an increased complexity at the receiver. The transmitter is based on the so-called Time Hopping UWB (TH-UWB) scheme while the receiver is a RAKE receiver with five branches. IR-UWB also provides good multipath properties, secure transmission, and accurate positioning with the latter being the main focus of this report.

Four positioning methods are presented with a view on finding which is the most suitable for UWB signaling. Received Signal Strength (RSS), Angle Of Arrival (AOA), Time Of Arrival (TOA) and Time Difference Of Arrival (TDOA) are all considered, and TDOA is found to be the most appropriate. Increasing the SNR or the effective bandwidth increases the accuracy of the time based positioning schemes. TDOA thus exploits the large bandwidth of UWB signals to achieve more accurate positioning in addition to synchronization advantages over TOA.

The TDOA positioning scheme is tested under realistic conditions and the results are provided. A sensor network is simulated based on indications provided by WesternGeco. Each sensor consists of a transmitter and receiver which generate and receive signals transmitted over a channel modeled after the IEEE 802.15.SG3 channel model. It is shown that the transmitter power and sampling frequency, the distance between the nodes and the position of

the target node all influence the accuracy of the positioning scheme. For a common sampling frequency of 55 GHz, power levels of -10 dBm, -7.5 dBm and -5 dBm are needed in order to achieve satisfactory positioning at distances of 8, 12, and 15 meters respectively. The need for choosing appropriate reference nodes for the cases when the target node is selected on the edges of the network is also pointed out.

Preface

This report has been written to satisfy the final thesis requirements in the 10th semester of the Master of Science study program of Electronics, at the Norwegian University of Science and Technology (NTNU). The teaching supervisors were Daniel Golparian at WesternGeco and Geir Øien at NTNU.

Trondheim, October 12, 2007

Senad Canovic

List of Acronyms

A/D - Analog/Digital

AOA - Angle of Arrival

ARAKE - All RAKE

AWGN - Additive White Gaussian Noise

CRLB - Cramer-Rao Lower Bound

DLL - Delay-Lock-Loop

DS - Direct-Sequence

DS-UWB - Direct-Sequence Ultra Wideband

EGC - Equal Gain Combining

ESD - Energy Spectral Density

FCC - Federal Communications Commission

GPS - Global Positioning System

IEEE - Institute of Electrical and Electronics Engineers

IR - Impulse Radio

IR-UWB - Impulse Radio Ultra Wideband

LOS - Line of Sight

LSE - Least Square Error

MB - Multi-Band

MBOA - MultiBand OFDM Alliance

MB-OFDM - Multi-Band Orthogonal Frequency Division Multiplexing

MB-UWB - Multi-Band Ultra Wideband
ML - Maximum Likelihood
MRC - Maximum Ratio Combining
NLOS - Non Line of Sight
OFDM - Orthogonal Frequency Division Multiplexing
PAM - Pulse Amplitude Modulation
PPM - Pulse Position Modulation
PPM-TH-UWB - Pulse Position Modulation Time-Hopping Ultra Wideband
PRAKE - Partial RAKE
PSD - Power Spectral Density
RSS - Received Signal Strength
SD - Selection Diversity
SNR - Signal to Noise Ratio
SRAKE - Selective RAKE
TH - Time-Hopping
TH-UWB - Time-Hopping Ultra Wideband
TDOA - Time Difference of Arrival
TOA - Time Of Arrival
UWB - Ultra Wideband

Contents

List of Figures	VI
List of Tables	VIII
1 Introduction	1
2 Ultra Wideband	3
2.1 Impulse Radio UWB	6
2.1.1 TH-UWB	7
2.1.2 DS-UWB	8
2.2 Multi-Band UWB	9
2.3 The RAKE receiver	10
2.4 Characteristics of UWB signals	12
3 Position estimation and UWB	14
3.1 Ranging and positioning techniques	17
3.1.1 Time of Arrival (TOA)	17
3.1.2 Time Difference of Arrival (TDOA)	23
3.1.3 Received Signal Strength (RSS)	24
3.1.4 Angle of Arrival (AOA)	25
3.2 Comparison of the positioning techniques from the viewpoint of a UWB system	26
4 Simulations, results and discussions	28
4.1 Description of the simulation process	28
4.1.1 The Channel model	31
4.2 Simulation scenarios	33
4.2.1 Power and sampling frequency variations	33
4.2.2 Distance between the nodes	36
4.2.3 Position of target node	37

5	Conclusions	46
5.1	Future work	48
	Bibliography	50
A	Appendix	I
A.1	IEEE 802.15.SG3 channel model parameters	I
A.2	MATLAB files	II
A.2.1	<i>Posisjonering_hovedfil.m</i>	II
A.2.2	<i>posisjonering.m</i>	VI
A.2.3	<i>kanalmodell2.m</i>	X
A.2.4	<i>cp0802_IEEEubLOS4.m</i>	XIII
A.2.5	<i>cp0801_Gnoise_mod.m</i>	XVII
A.2.6	<i>cp0201_transmitter_2PPM_TH_2</i>	XIX
A.2.7	<i>cp0201_transmitter_2PPM_TH_3</i>	XXIII

List of Figures

2.1	Power spectral density for UWB, wideband and narrowband signals	3
2.2	FCC emission mask for UWB indoor and handheld/outdoor devices respectively(FCC, 2002).	5
2.3	PSD for higher order differentiated Gaussian pulses.	6
2.4	Schematization of the generation process for PPM-TH-UWB	8
2.5	Schematization of the generation process for PAM-DS-UWB	9
2.6	Frequency band division according to MBOA	10
2.7	A RAKE receiver structure for TH-IR-UWB systems	11
3.1	Node-centered positioning	15
3.2	Relative positioning	16
3.3	Perfect delay estimation	19
3.4	Spherical positioning	21
3.5	AOA positioning. The green nodes are the reference nodes.	26
4.1	The sensor network imagined by WesternGeco	29
4.2	The nucleus consisting of seven nodes	29
4.3	The result of the positioning scheme for a distance of 7 m and an available power of -20 dBm	34
4.4	The result of the positioning scheme for a distance of 7 m and an available power of -5 dBm	35
4.5	Sensors that can be positioned as centres of a nucleus	37
4.6	The result of the positioning scheme when the target node is at the edge of the nucleus.	39
4.7	The result of the positioning scheme when the nodes farthest off are discarded	40
4.8	Sensors at the edges that can be found by using only three reference nodes.	41
4.9	Positioning scheme when two reference nodes are discarded.	42

4.10	Sensors that can be positioned by the use of the methods described thus far.	43
4.11	The third reference node is a non-neighbouring sensor.	44
4.12	Proposed positions for the two sensors to be added.	45
A.1	Parameters for the IEEE 802.15.SG3 channel model	I

List of Tables

4.1	Effects of power variation on the positioning accuracy.	33
4.2	Effects of distance variation on the positioning accuracy.	36
4.3	Optimal distance between the nodes.	37
4.4	Positioning error when the target node is set to the edge of the nucleus.	38
4.5	Positioning error when the nodes farthest off are discarded and only three reference nodes are used.	38
4.6	Positioning results when four reference nodes are used.	41
4.7	Positioning results when the nearest non-neighbouring sensor is selected as the third reference node.	43

Chapter 1

Introduction

Sensor networks have widespread uses for many purposes. Companies like WesternGeco use sensor networks in their seismic operations all around the world. These operations may consist of searching for oil and other natural resources in a variety of different terrain types. Unfortunately, operating such networks in some terrains, like the jungles of South America, may be quite challenging. Positioning is the process of determining the positions of the sensors in a network. Automatic localization of sensors in a wireless sensor network is a necessity since the location of a sensor must be known for its data to be meaningful. This knowledge in turn enables such services as emergency target identification and tracking, location dependent computing and geographic routing provided that the positioning information is accurate enough [1]. A straight forward solution for positioning is usually to implement GPS chipset/modules on each sensor unit. Terrain types like the one mentioned above have poor GPS coverage and only a few units are able to receive proper coverage.

Sensor networks combine information from multiple nodes in order to refine a position estimate. A sensor node can not choose its location and must deal with nonideal propagation conditions which affect the ranging measurements [2]. The nature of UWB signals with their wide bandwidth provides excellent opportunities for range estimation and positioning under nonideal conditions [3]. A lot of research has already been done on this area and some IEEE Task Groups (such as IEEE 802.15.4a) are currently working on such issues.

A study of the UWB technology and the advantages and disadvantages as-

sociated with this will be presented. Methods and principles for positioning using UWB technology will be identified. The most suitable method will then be tested under realistic conditions in order to draw conclusions on how well it is suited for positioning in the networks imagined by WesternGeco.

Chapter 2

Ultra Wideband

Ultra Wideband (UWB) is presently a rapidly developing technology. It all started in 2002 when the *Federal Communications Commission (FCC)* in the USA allocated the spectrum for UWB[4]. This was a large frequency spectrum that was to be used at a very low power. The low power spectral density of UWB avoids interference with underlying narrowband and wideband signals and allows UWB to coexist with the latter.

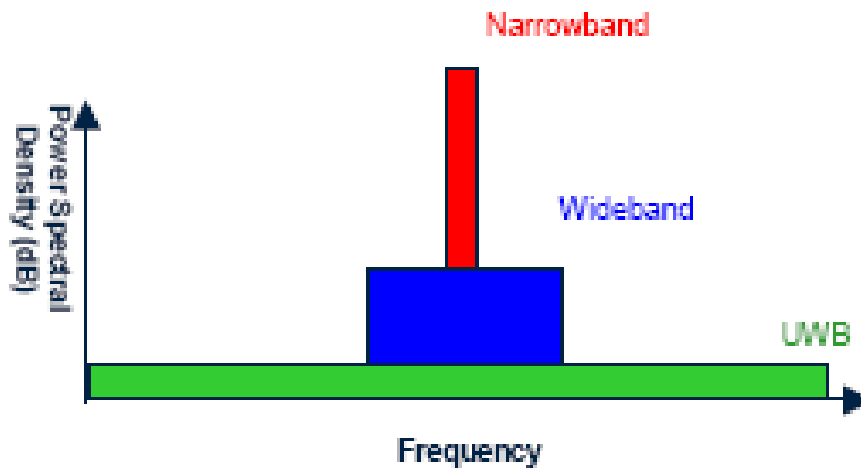


Figure 2.1: Power spectral density for UWB, wideband and narrowband signals

UWB bandwidth exists in the 3100 MHz-10600 MHz frequency range with an

allowed power of -41 dBm/MHz[5]. UWB is defined as transmission systems that either have a -10 dB *fractional bandwidth* larger than 0.20 or have an -10 dB bandwidth larger than 500 MHz. *Fractional bandwidth*, here denoted as B_{fract} , is defined as the ratio of the total bandwidth B of the signal to the center frequency f_c . This can be mathematically described as:

$$B_{fract} = \frac{(f_H - f_L)}{\left(\frac{f_H + f_L}{2}\right)} \quad (2.1)$$

According to [3], UWB has traditionally been emitted by radiating pulses that are very short in time, typically a few nanoseconds. This technique is called *Impulse Radio* (IR) and was originally used in military radar applications. When the frequency band for UWB was allocated in 2002 there was a significant interest in applying this technology to wireless communication. There was an disagreement however in whether one should use a standard based on the old IR-technique or on continuous carrier waves. Today there are mainly two UWB technologies that are receiving a significant amount of attention, IR-UWB and *Multi-Band* (MB) UWB, which uses frequency hopping with *Orthogonal Frequency Division Multiplexing*(OFDM)[6]. IR-UWB can be further subcategorized in *Time-Hopping*(TH) UWB and *Direct-Sequence*(DS) UWB. In this assignment the main focus will be at the use of IR-UWB as a communication tool for positioning and ranging between sensors when incorporated in the different positioning methods. The reason is the superior amount of literature available on IR-UWB and positioning compared to MB-OFDM. However, a short description of MB-OFDM will be presented as to provide a short overview of UWB-technology today.

The main challenge concerning UWB technology is using all the available bandwidth without exceeding the boundaries set by the FCC. This is discussed in [3] and [5] and will be presented in the following text. Impulse based UWB usually offers only one physical channel and in order to transmit to maximum effect it is imperative that this channel covers the available spectrum as completely as possible. A signal that perfectly "fills" the available 3,1 GHz - 10,6 GHz bandwidth gives a maximum transmission power of 0.55mW (-2.6dBm) when integration over the FCC mask is performed. The spectrum of the transmitted signal will depend on the pulse shape of the signal and how the pulses are placed in the time domain. The most common pulse shapes are different variations of Gaussian pulses. The Gaussian pulse can

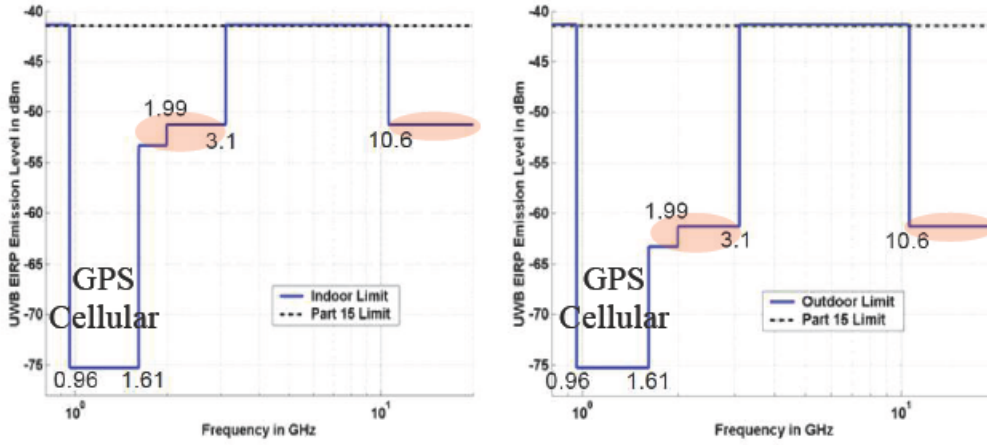


Figure 2.2: FCC emission mask for UWB indoor and handheld/outdoor devices respectively(FCC, 2002).

be expressed by:

$$p(t) = \pm \frac{1}{\sqrt{2\pi\sigma^2}} e^{-\left(\frac{t^2}{2\sigma^2}\right)} = \pm \frac{\sqrt{2}}{\alpha} e^{-\left(\frac{2\pi t^2}{\alpha^2}\right)} \quad (2.2)$$

where $\alpha^2 = 4\pi\sigma^2$ is the shape factor and σ^2 is the variance. It can be observed that a reduction of α will lead to shorter pulses and consequently to a larger bandwidth of the emitted signal. The power spectrum of a signal consisting of consecutive Gaussian pulses will consist of several low-power spectral lines. These will have an envelope restricted by the boundaries of an envelope of the power spectrum of a single Gaussian pulse. Random spreading sequences such as TH and DS can then be used in order to achieve multiple user access and a certain "smoothing" of the power spectrum. This "smoothing" is a result of the increased number of spectral lines that are dispersed around the available frequency band. These harmonic components will move a certain amount of power away from the tops and out to other parts of the band. Since the FCC mask shown in Figure 2.2, only limits the power (average energy) radiated, a certain increase in the power of the emitted pulses can be achieved with the use of spreading sequences without stepping out of the FCC mask.

In order to fill the available spectrum in a best possible way it is important that the center frequency, f_c , is placed appropriately in the emission mask. By differentiating the Gaussian pulse, the center frequency of the emitted signal can be altered. This is shown in figure 2.3 where the center frequency is increased with increasing differentiation order of the pulse [3].

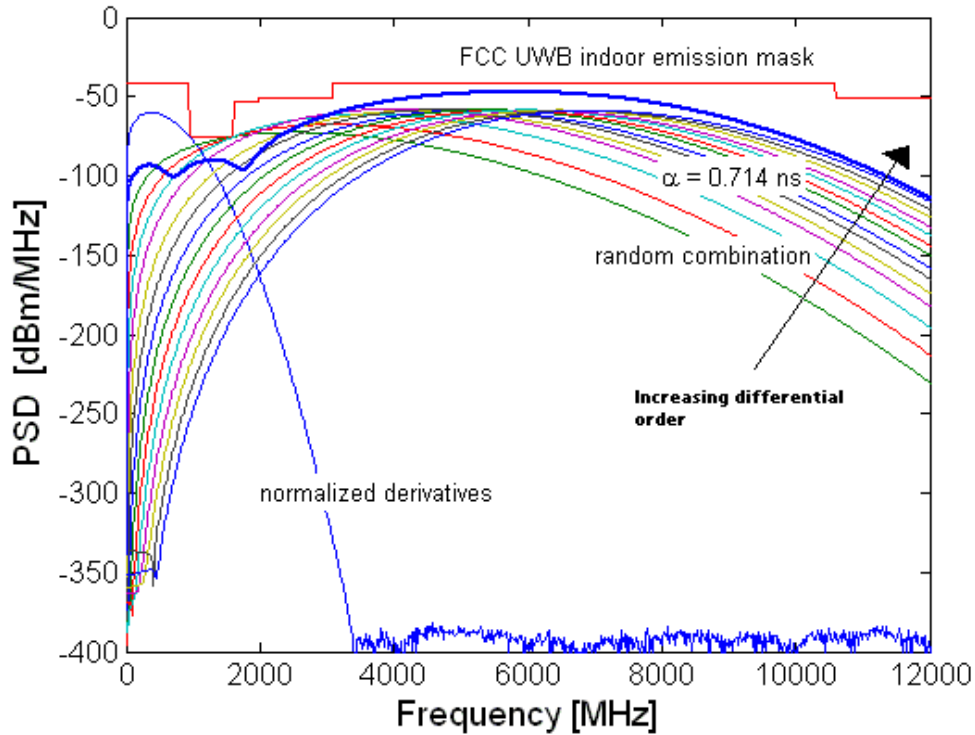


Figure 2.3: PSD for higher order differentiated Gaussian pulses.

The instant transmission power can not be increased in a similar way as described earlier if periodic pulses were to be used. Even though the energy of the pulses can be increased, the shape of the pulses would still set the same limitations regarding peak frequency and bandwidth.[5]

2.1 Impulse Radio UWB

The most common way of emitting UWB-signals is by generating pulses that are very short in time (a few nanoseconds) and then emitting them at a very high data rate[5]. The information data symbols modulate the pulses by different methods. *Pulse Position Modulation (PPM)* and *Pulse*

Amplitude Modulation (PAM) are commonly adopted modulation schemes. TH-UWB and DS-UWB can in principle adopt either PPM or PAM for data modulation[3]. A specific modulation method might however be more appropriate in some cases for one or the other according to spectrum shapes and characteristics. A description of the generation process of the two previously mentioned IR-UWB techniques will now be given. A RAKE receiver will also be presented in order to describe a full UWB transmitter/receiver scheme.

2.1.1 TH-UWB

In this section TH-UWB combined with PPM will be described. The information presented is gathered from [3] and [7]. Figure 2.4 shows the generation scheme for this type of UWB-signals. The process starts at the first block which is the **repetition coder**. A binary sequence \mathbf{b} is generated at a rate of $R_b = 1/T_b$ bits/s and the repetition coder repeats each bit N_s times and generates a binary sequence \mathbf{a} at a rate of $R_{cb} = N_s/T_b = 1/T_s$ bits/s, where T_s is the frame time. Redundancy is introduced in this way and the system is seen as an $(N_s, 1)$ repetition coder.

The **transmission coder** in the second block generates a new sequence \mathbf{d} by applying an integer-valued code \mathbf{c} to the previously generated sequence \mathbf{a} . This code introduces a TH shift on the generated signal and thus brings the TH in TH-UWB. This gives the generic element of \mathbf{d} which can be expressed as $d_j = c_j T_c + a_j \epsilon$, where T_c is the chip time and ϵ is the PPM shift. These two elements are constant terms that satisfy the condition $c_j T_c + \epsilon < T_s$. In general, $\epsilon < T_c$ is also the case, and it is also important to note that \mathbf{d} is a real-valued sequence while \mathbf{b} and \mathbf{c} are binary and integer-valued respectively.

The third block is the **PPM modulator**. It receives the sequence \mathbf{d} and produces a series of Dirac pulses ($\delta(t)$) at the rate $R_p = N_s/T_b = 1/T_s$. These pulses occur at times $(jT_s + c_j T_c + a_j \epsilon)$ and are, as it can be seen, shifted in time from the nominal position jT_s by $d_j = c_j T_c + a_j \epsilon$.

The last part of the process is the shaping of the generated pulses. This is done in the **Pulse Shaper** which has an impulse response $p(t)$. The clue here is to shape the pulses in such a way that they become strictly non-overlapping while the available bandwidth is utilized in the best possible way [7]. This implies meeting the emission masks set by regulation authorities such as the FCC.

At the end of the generating process we get the final expression for a PPM-

TH-UWB signal:

$$s(t) = \sum_{-\infty}^{\infty} p(t - jT_s + c_j T_c + a_j \epsilon) \quad (2.3)$$

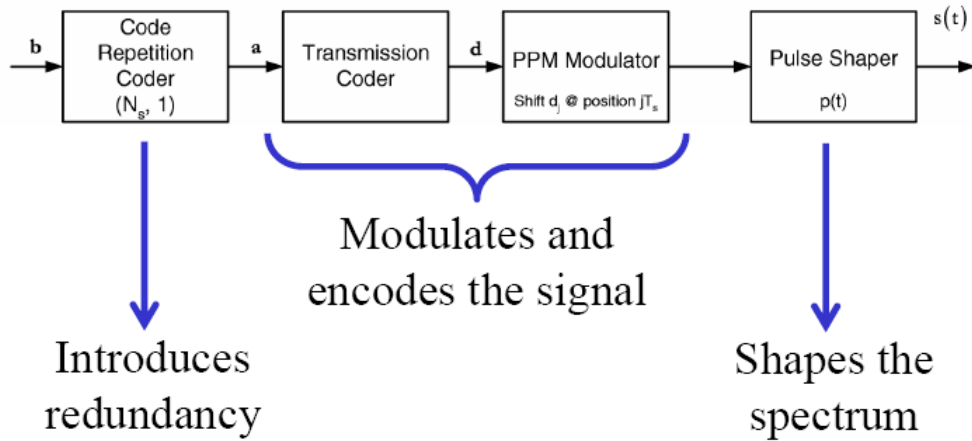


Figure 2.4: Schematization of the generation process for PPM-TH-UWB

2.1.2 DS-UWB

The generation of DS-UWB signals starts in the same way as for the previously described TH-UWB. The theory presented in this section has been gathered from [3] and [8]. A binary sequence is generated at the same rate, $R_b = 1/T_b$, and the first part of the system is a **repetition coder** which repeats each bit N_s times and generates a new binary bit sequence a^* at a rate of $R_{cb} = N_s/T_b = 1/T_s$ bits/s. Redundancy is also introduced in this way.

The next step is the **binary series** part of the system where the sequence a^* is transformed into \mathbf{a} which is composed of binary antipodal symbols (± 1). This sequence then enters the **transmission coder** which applies a binary code \mathbf{c} consisting of (± 1)'s and with period N_p to the sequence \mathbf{a} . A new sequence $\mathbf{d} = \mathbf{a} * \mathbf{c}$ is generated, consisting of $d_j = a_j c_j$.

Sequence \mathbf{d} then enters the **PAM-modulator** where a sequence of Dirac pulses ($\delta(t)$) positioned at jT_s is generated at a rate $R_p = N_s/T_b = 1/T_s$.

The train of Dirac pulses enters the **pulse shaper** as a last part of the generating process. The shaper has the same function here as the case was with TH-UWB. Its main task is making sure that the output is a sequence of strictly non-overlapping pulses.

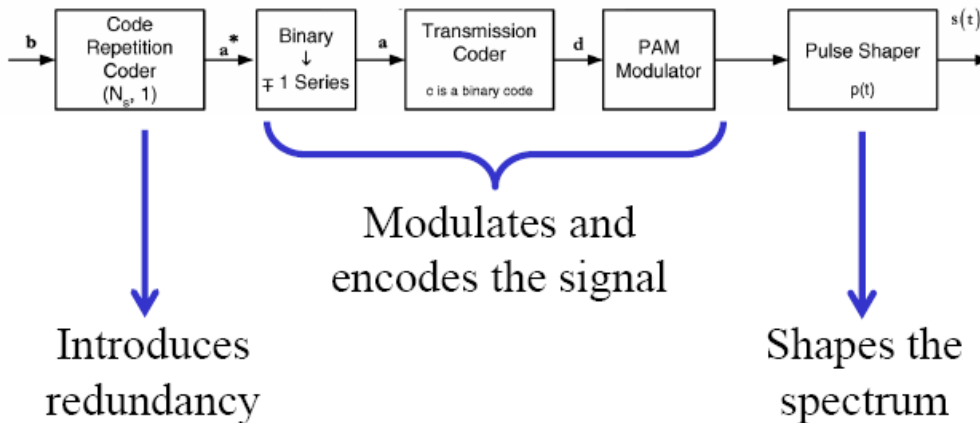


Figure 2.5: Schematization of the generation process for PAM-DS-UWB

2.2 Multi-Band UWB

Multi-Band UWB is a method fundamentally different than IR-UWB. A short description will be given in this section. Due to the inferior amount of literature on research regarding MB-UWB compared to IR-UWB, the focus of this assignment is biased towards IR-UWB. This chapter is merely supposed to give a short description of MB-UWB and thus in short terms describe an alternative way of thinking UWB.

The frequency spectrum allocated to UWB in the US by the FCC was set to 3.1 GHz - 10.6 GHz. The MB-UWB principle consists of dividing the available 7.5 GHz bandwidth into smaller frequency bands of at least 500 MHz each[8]. It is then possible to implement only parts of the available spectrum. The possibility to dynamically operate on only parts of the available spectrum is of great importance since the laws for frequency allocation vary worldwide. The transmission of data occurs on different subbands and interference can thus be avoided in certain bands.

There are several types of modulation schemes that can be applied within each of the respective bands. Orthogonal Frequency Division Multiplexing (OFDM) is however the most common [5]. The MultiBand OFDM Alliance (MBOA) is an worldwide organization consisting of more than 60 leading companies that support a single technical proposal for MB-UWB. In the MBOA approach, the available 7,5 GHz spectrum is divided into subbands that are 528 MHz each. The band plan proposes five logical channels where Channel 1 contains the first three bands and is mandatory for all UWB devices. The four other channels are optional.

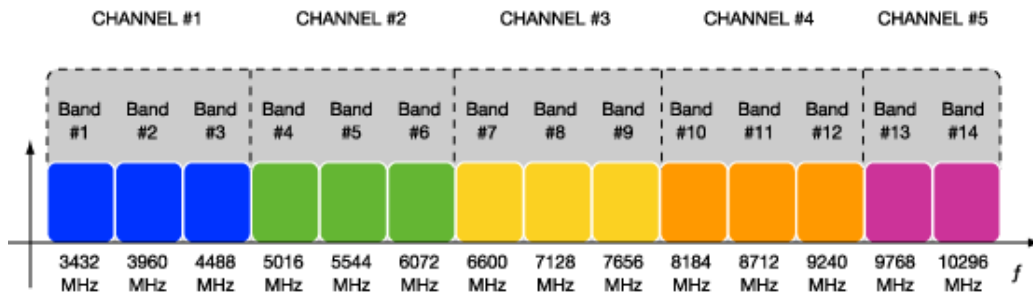


Figure 2.6: Frequency band division according to MBOA

2.3 The RAKE receiver

RAKE receivers are often used in connection with UWB in order to exploit the multipath properties of the UWB signals [9]. This is the case since the overall received energy of a transmitted pulse, E_r , is spread in time with the different multipath contributions. If the time delay of the various multipath contributions is smaller than the pulse duration T_m , the signal contributions overlap and are not independent. This means that an amplitude observed at a time t is affected by multipath components arriving just before or after time t . The number of independent paths thus depends on T_m . The smaller T_m , the higher number of independent contributions at the receiver input. IR-UWB systems produce pulses that are quite short, in the order of nanoseconds, which leads to the assumption that all multipath contributions are non-overlapping. This means that IR-UWB systems can in principle take advantage of multipath propagation by combining a large number of different and independent replicas of the same transmitted pulse [3].

The name RAKE comes from the notion that the multibranch receiver resembles a rake where each of its fingers are branches in the receiver that receive different multipath components [10]. These branches consist of a bank of correlators or matched filters. Each branch is matched to a different multipath component and these are then combined in order to maximize receiver performance. Figure 2.7 shows the structure of a RAKE receiver where r_{rx} is the received signal, L is the number of correlators (the number of multipath contributions to be considered), τ_L is the time delay of the L 'th multipath contribution, v_{temp} is the correlated signal and β_L is the weighing factor for branch L .

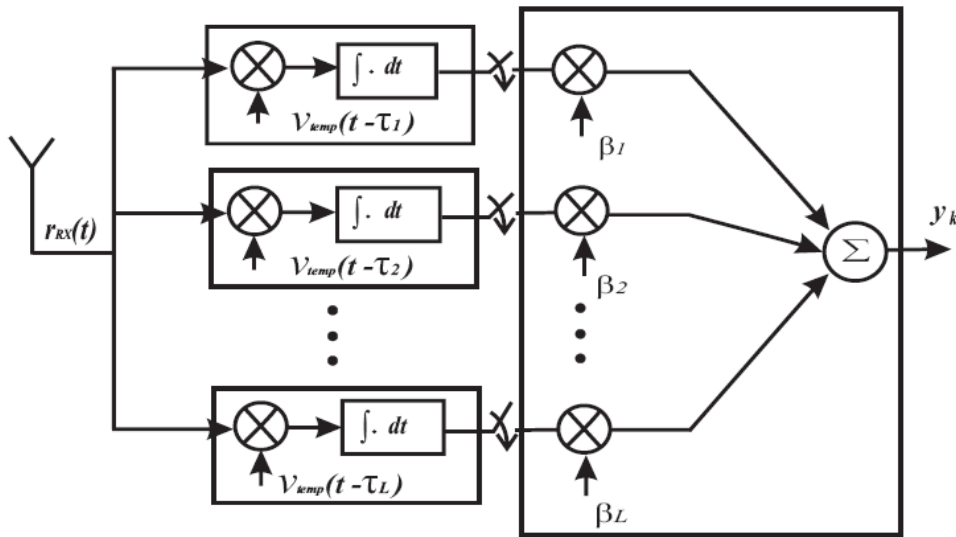


Figure 2.7: A RAKE receiver structure for TH-IR-UWB systems

If the receiver uses all available paths it is called an all RAKE (ARAKE). This is however usually not the case. The number of multipath components that can be utilised is limited by the power consumption, designer complexity and the channel estimation. Selective RAKE (SRAKE) and partial RAKE (PRAKE) use only a limited number of branches and thus exploit only some of the multipath components at the receiver. Partial RAKE uses the M first arriving paths out of a number L of resolvable multipath components. The selective RAKE however, searches for the M best paths out of L received multipath components. This method is called Maximum Ratio Combining (MRC)[9]. Other strategies for exploiting diversity are the Selection Diversity

(SD) and the Equal Gain Combining (EGC). These are based on selecting the multipath contribution with the best signal quality and operating on this one only, or aligning the different contributions in time and adding without any particular weighing, respectively [3]. The RAKE is essentially a form of diversity combining where several paths a signal takes from a transmitter to a receiver are used to achieve as high signal strength and quality at the receiver as possible. [10]

2.4 Characteristics of UWB signals

UWB is a promising technology with great potential, but as every other technology, it has its advantages and drawbacks. These are discussed thoroughly in [11], [5] and [3] and the results are presented in this section. The main advantage of UWB is obviously the large available bandwidth. According to Shannon's channel capacity theorem, a larger bandwidth will theoretically have a positive effect on the total channel capacity. For a more thorough investigation of UWB and its influence on channel capacity, the reader is referred to [12]. The high data rate also makes room for a high flexibility regarding UWB. Some of the data rate can be traded for longer range or more robust operation.

Additionally, a large bandwidth improves reliability as the signal contains different frequency components which increases the possibility that at least some of them will go through and around obstacles.

Furthermore, the large bandwidth of UWB offers improved ranging and positioning accuracy. This will be further discussed in subsequent chapters. Regarding communication, large bandwidths tend to alleviate smallscale fading.

IR-UWB consists of single, consecutive pulses. These are fairly easy to generate by employing time delays and thus enable low-power transmitters. The spreading of the pulses over a large bandwidth, and the subsequent lowering of the power spectral density (PSD), reduce interference to other systems. UWB operates at a PSD that is usually lower than the noise from the environment. This allows coexistence with narrowband users and increases security as the possibility of interception is reduced. The receiver must be aware of the pulse allocation in order to decode the signal.

Channel allocation by means of TH and DS combined with the short time duration of the pulses allows many channels to operate simultaneously with small fears of pulse collisions. By supplying transmitters with different TH and DS sequences interference between transmitters can be reduced to an

insignificant level.

There are some disadvantages to UWB that need to be addressed. IR-UWB allocates channels by means of TH or DS. This is a relatively time-consuming process since there are strict requirements regarding synchronization between the transmitter and receiver.

The receivers pose one of the largest challenges concerning UWB at the present time. A/D converters and digital signal processors are needed due to the large frequency components. According to the Nyquist theorem [13], in order to avoid aliasing, the sampling frequency needs to be at least twice the size of the largest frequency component. When operating at a frequency band of 3.1 GHz - 10.6 GHz, the sampling frequency must be at least $2 \cdot 10.6 \text{ GHz} = 21,2 \text{ GHz}$. This makes the construction of a low-power receiver a challenge. Another drawback to UWB is the relatively short range of 10-20 m due to the power-regulations set by the FCC.

Chapter 3

Position estimation and UWB

The ability to localize sensors in a network is crucial when dealing with networks which monitor certain geographical areas and terrain types. Resource sharing and routing can be optimized when positioning information is available throughout the network. Knowing how to locate static and if need be moving objects with high precision is thus an extremely appealing feature in the design of wireless networks. Different ranging and positioning techniques are used to achieve this. The terms *ranging* and *positioning* are often used in contrasting ways in the available literature and will therefore be defined shortly before a more detailed description of the techniques for achieving these is given. The information gathered from the other literature that is mentioned further on will be adapted to these definitions. The definitions are based on the ones made in [3] and most of the theory presented in chapter 3 is thus based on [3]. Other sources of information will be mentioned separately.

Ranging is defined as finding the distance between a target node and a reference node within a network. These distances are then used to determine the position of the target node. This is called **positioning** and can be seen as "advanced ranging". Positioning can be subcategorized in node-centered, relative and absolute positioning. *Node-centered positioning* is defined as the action of computing the positions of a set of target nodes with respect to a reference node. Any given node can be viewed as a reference node and the positions of the other nodes can be found referenced to this one.

When it comes to *relative positioning* the key notion is that the positions of a set of nodes are calculated with respect to a common system of coordinates.

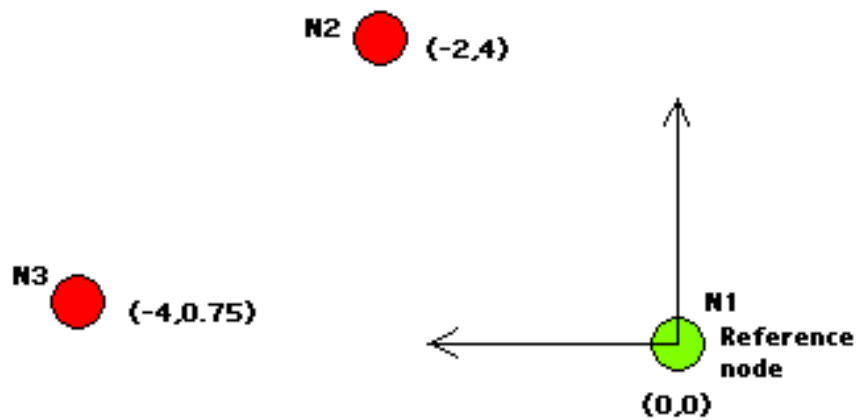


Figure 3.1: Node-centered positioning

All nodes share the same reference system and each node has a unique set of coordinates within this system. The reference coordinate system can be placed arbitrarily but evolves typically from the node-centered system where it coincides with the coordinate system of a given node.

Absolute (geographical) positioning is a special case of relative positioning that is worth mentioning. The reference coordinate system coincides in this case with the global coordinate system in which the coordinates are given in terms of latitude and longitude and are unique worldwide for each node.

The terms *ranging* and *positioning* are equally important for localizing sensors in a given network. Accuracy in distance estimation is necessary in order to achieve accurate positioning [14]. There are several techniques that can help in localizing nodes accurately and they will be presented in the following chapters. How adaptable each of the different techniques is to UWB signaling will be assessed, and a comparison will be made between the methods as to find the most suitable.

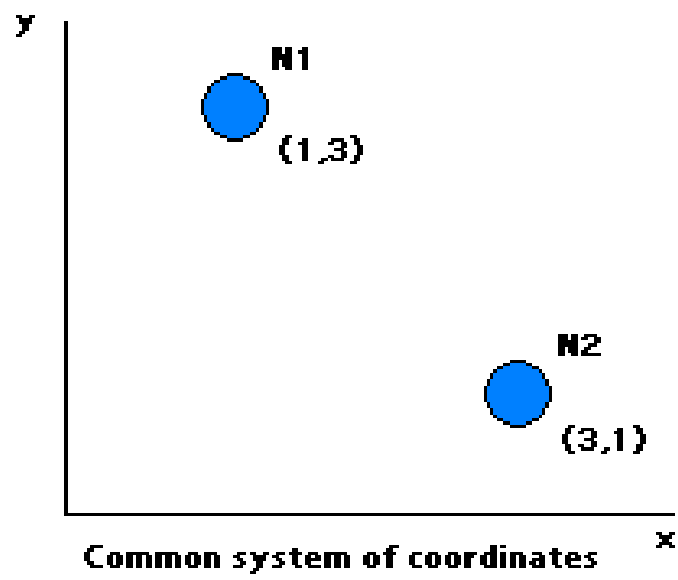


Figure 3.2: Relative positioning

3.1 Ranging and positioning techniques

Since ranging is an integral part of positioning, some of the techniques that are to be described in this chapter can be viewed as both ranging and positioning techniques. Time of arrival (TOA) is the most commonly used distance estimation method in the radar field and the terms "*TOA*" and "*ranging*" are often interchanged. One can at the same time argue that TOA is a positioning method, as will be described shortly.

3.1.1 Time of Arrival (TOA)

Time of arrival is a popular method for node localizing. It can, as mentioned earlier, be viewed as a both ranging and positioning method. Ranging is the first step of a positioning scheme and the use of TOA in both will be described in this section. Most of the theory presented is gathered from [3] and supplemented with other literature.

The TOA technique uses an estimation of the propagation delay between transmitter and receiver to compute the distance in between. The received signal can be mathematically described as

$$r(t) = \alpha s(t - \tau_d) + n(t) \quad (3.1)$$

where α and τ_d are attenuation and delay respectively, while $n(t)$ is AWGN. TOA uses τ_d to estimate the delay. Accurate delay estimation is important in wireless communications in order to achieve symbol synchronization between transmitter and receiver.

The **Maximum Likelihood (ML)** estimator is commonly used throughout the literature in order to achieve satisfactory estimation of the arrival time delay [15]. This can be achieved by finding the value of τ_d that maximizes the correlation between the received signal $x(t)$ and sent signal $s(t)$. The correlation function is defined as follows:

$$r_{xs}(\tau_d) = \frac{1}{T_0} \int_{T_0} x(t)s(t - \tau_d)dt \quad (3.2)$$

where T_0 is the auto-correlation duration, which is equal to $\frac{T_p}{2}$ where T_p is the pulse width.

The TOA technique however, finds the distance by estimating the propagation delay between transmitter and receiver with the help of the ML estimator. The maximum likelihood estimate of delay τ is defined as follows:

$$\hat{\tau}_{ML}(r) = \operatorname{argmin}_{\tau \in \mathbb{R}} \left(e^{\frac{-1}{N_0} \int_{T_{obs}} (r(t) - s(t-\tau))^2 dt} \right) \quad (3.3)$$

where N_0 is the Power Spectral Density (PSD) of the noise, and T_{obs} is the observation interval over which the estimation is performed.

There are several ways to find the desired propagation delay τ . The so called *early-late gate synchronizer* is a common scheme that can be used when a common time reference between sender and receiver is available. The demand of a common reference exists so that the propagation delay can be isolated as the only delay. The output $R_s(\xi)$ of a filter matched to an input signal $s(t)$ at a receiver is triangular shaped with a peak obtained by sampling $R_s(\xi)$ at $\xi=T$. The early-late gate synchronizer exploits the symmetry of $R_s(\xi)$ by extracting two values from the signal at symmetrical positions around the expected peak value. This is done by sampling $R_s(\xi)$ at $\xi = T - \delta$ and $\xi = T + \delta$ respectively. The following equation is then evaluated:

$$\Delta R_s = R_s(T - \delta) - R_s(T + \delta) \quad (3.4)$$

In the case of $\Delta R=0$, the two samples are identical and TOA is perfectly estimated, as shown in Figure 3.3. The two other options are $\Delta R_s < 0$ and $\Delta R_s > 0$. These represent imperfect TOA estimation where the two samples of $R_s(\xi)$ are not identical. In the case of $\Delta R_s < 0$ the estimated TOA is smaller than the actual TOA. This can be adjusted by introducing an additional delay which is proportional to $\Delta |R_s|$. When $\Delta R_s > 0$ the TOA estimate must be adjusted by decreasing the estimate of a quantity which is proportional to $\Delta |R_s|$. The additional delay that is introduced until $\Delta R_s = 0$ is achieved, represents the desired estimation of the random delay τ .

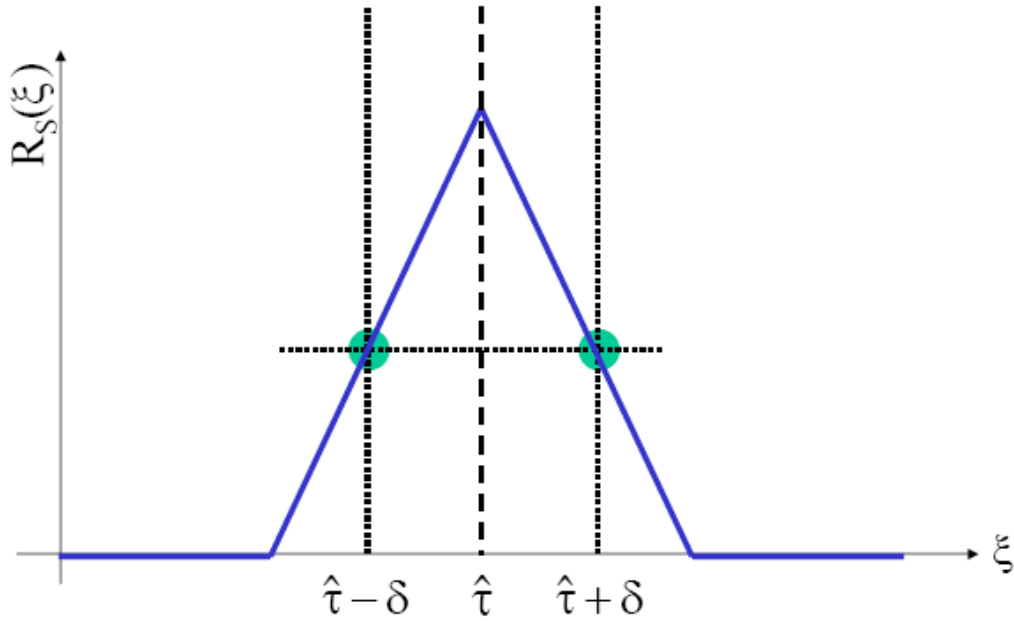


Figure 3.3: Perfect delay estimation

In order to achieve synchronization when working with ranging estimation between nodes without a common time reference between sender and receiver it is necessary to introduce a handshake protocol. Communication and delay estimation between two nodes $N1$ and $N2$ will then be conducted as follows. $N1$ sends a packet at a time t_0 . This is received by the target node $N2$ at a time $t_0 + \tau$ where τ is the propagation delay between the two nodes. $N2$ then replies according to ranging procedure with an identical packet sent at a time $t_0 + \tau + \Delta$. Δ represents a fixed time delay which is known to both transmitter and receiver and takes into account processing delays in the target node. $N1$ receives the packet at a time $t_1 = t_0 + \tau + \Delta + \tau$. The propagation delay can finally be expressed by the following equation:

$$\tau = \frac{t_1 - t_0 - \Delta}{2} \quad (3.5)$$

The propagation delay τ can then be used to calculate the distance between the two nodes. This is done by multiplying τ with the speed of light, c [14],

as expressed in the following Equation:

$$d = \tau \cdot c \quad (3.6)$$

$\hat{\tau}_{ML}$ corresponds to the τ value which minimizes the ML function in the case of AWGN, $n(t)$. The accuracy of the TOA estimation is expressed by the variance of the TOA estimation error $\sigma_{\hat{\tau}}^2$ which is related to the bandwidth and SNR at the receiver. ML theory tells us that the lower limit for $\sigma_{\hat{\tau}}^2$ is given by the Cramer-Rao lower bound (CRLB) [14]:

$$\sigma_{\hat{\tau}}^2 = \frac{N_0}{2 \int_{-\infty}^{+\infty} (2\pi f)^2 |P(f)|^2 df} \quad (3.7)$$

Here, $|P(f)|^2$ is the bilateral Energy Spectral Density (ESD) of the UWB pulse $p(t)$. ESD can be expressed as:

$$|P(f)|^2 = \begin{cases} G_0 & \text{for } f \in [f_L, f_H] \cup [-f_H, -f_L] \\ 0 & \text{outside} \end{cases} \quad (3.8)$$

Combining Equations 3.7 and 3.8 gives a new expression for $\sigma_{\hat{\tau}}^2$ that can be written as:

$$\sigma_{\hat{\tau}}^2 = \frac{N_0}{\frac{8}{3}\pi^2 2G_0 B (f_H^2 + f_H f_L + f_L^2)} \quad (3.9)$$

Here, B is the occupied bandwidth $B = (f_H - f_L)$. Equation 3.9 shows that the variance of the delay estimation is inversely proportional to the signal bandwidth occupation. A large bandwidth gives more accurate delay estimation and ranging results. This shows that the TOA technique is well suited for UWB radio because of the ultra-wide bandwidth.

It is however important to note that since the theoretical achievable accuracy under ideal conditions is quite large, clock synchronization between the nodes becomes an important factor to consider when TOA estimation is applied.

TOA is additionally seen as a positioning method often referred to as *spherical positioning*[3]. It is a continuation of the ranging measurements in the respect that both node-centered and relative positioning based on TOA require the ranging information in order to achieve successful positioning. The degree of accuracy in the received ranging information will have impact on the positioning accuracy. Successful ranging computations enable a given node N_i to know its distance from all other nodes. N_i can then choose k reference nodes (N_1, \dots, N_k) to set up a reference system in order to determine its position.

The spherical positioning scheme exploits the fact that in a tridimensional space (x,y,z) , the distance between a node to be positioned, N_i , and a reference node N_j , can be seen as a radius D_{ji} of a sphere centered in N_j . This information is then used to find the position of N_i by looking at the intersection point between the spheres (with radii D_{1i}, \dots, D_{ki}) of all reference nodes (N_1, \dots, N_k).

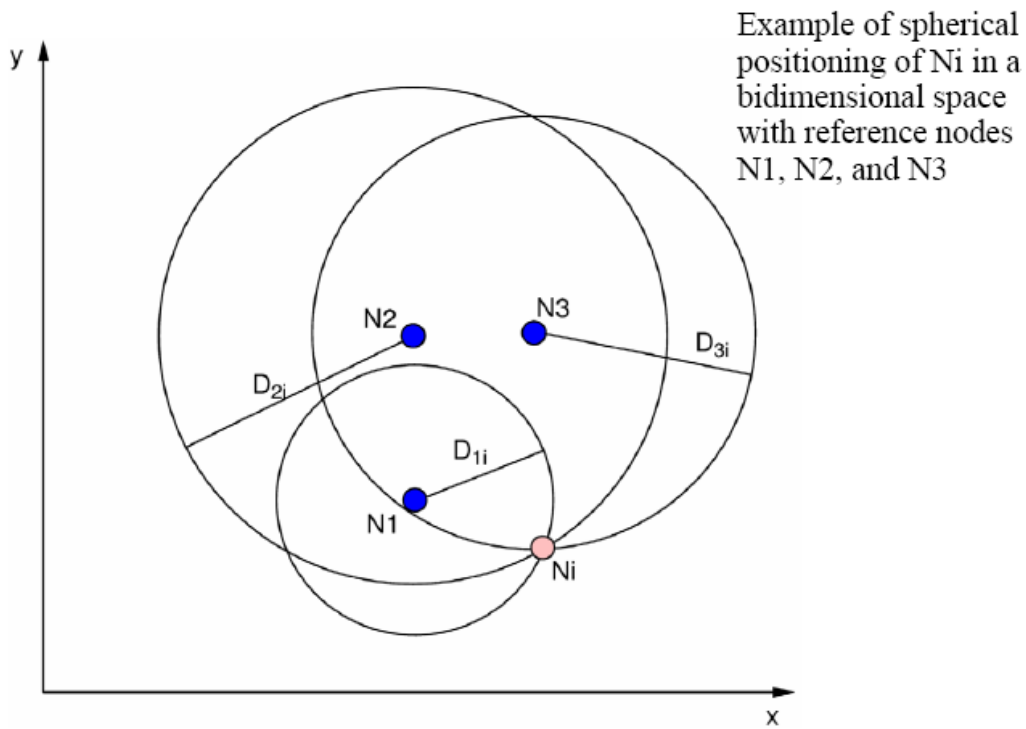


Figure 3.4: Spherical positioning

In order to achieve positioning in a three-dimensional space with perfect distance estimation it is necessary to have four reference nodes with a joint intersection point. However, it is useful to have additional reference nodes

available in order to improve positioning results in non-perfect distance estimation cases. In two-dimensional positioning only three reference nodes are needed with perfect distance estimation. The intersection between k spheres used for tridimensional positioning can be found by solving the following system of equations:

$$\left\{ \begin{array}{l} \sqrt{(X_1 - X_i)^2 + (Y_1 - Y_i)^2 + (Z_1 - Z_i)^2} \\ \sqrt{(X_2 - X_i)^2 + (Y_2 - Y_i)^2 + (Z_2 - Z_i)^2} \\ \vdots \\ \sqrt{(X_k - X_i)^2 + (Y_k - Y_i)^2 + (Z_k - Z_i)^2} \end{array} \right\} = \left\{ \begin{array}{l} D_{1i} \\ D_{2i} \\ \vdots \\ D_{ki} \end{array} \right\} \quad (3.10)$$

for $k \geq 4$.

The two-dimensional scheme can be expressed as follows:

$$\left\{ \begin{array}{l} \sqrt{(X_1 - X_i)^2 + (Y_1 - Y_i)^2} \\ \sqrt{(X_2 - X_i)^2 + (Y_2 - Y_i)^2} \\ \vdots \\ \sqrt{(X_k - X_i)^2 + (Y_k - Y_i)^2} \end{array} \right\} = \left\{ \begin{array}{l} D_{1i} \\ D_{2i} \\ \vdots \\ D_{ki} \end{array} \right\} \quad (3.11)$$

for $k \geq 3$.

Spherical positioning is a useful technique which can be used to localise nodes in a network. There are however some limitations regarding its use. TOA requires error-free ranging information in order to provide the position of the target node. This is often not the case in many practical situations where ranging estimates are affected by thermal noise and multipath while misalignments and clock drifts introduce random delays between clocks. In the presence of ranging errors an analytical solution of equation 3.10 which determines the position of node N_i may not exist. Minimization methods such as the Least Square Error (LSE) can be utilized in order to counter the effects of ranging errors. It is for this purpose convenient to rewrite equation 3.10 into a set of equations:

$$\bar{A}\bar{I} = \bar{b} \quad (3.12)$$

where

$$\bar{A} = -2 \begin{vmatrix} (X_1 - X_k) & (Y_1 - Y_k) & (Z_1 - Z_k) \\ (X_2 - X_k) & (Y_2 - Y_k) & (Z_2 - Z_k) \\ \vdots & \vdots & \vdots \\ (X_{k-1} - X_k) & (Y_{k-1} - Y_k) & (Z_{k-1} - Z_k) \end{vmatrix} \quad (3.13)$$

$$\bar{I} = \begin{vmatrix} X_i \\ Y_i \\ \vdots \\ Z_i \end{vmatrix} \quad (3.14)$$

and

$$\bar{b} = \begin{vmatrix} D_{1i}^2 - D_{ki}^2 - X_1^2 + X_k^2 - Y_1^2 + Y_k^2 - Z_1^2 + Z_k^2 \\ D_{2i}^2 - D_{ki}^2 - X_2^2 + X_k^2 - Y_2^2 + Y_k^2 - Z_2^2 + Z_k^2 \\ \vdots \\ D_{(k-1)i}^2 - D_{ki}^2 - X_{(k-1)i}^2 + X_k^2 - Y_{(k-1)i}^2 + Y_k^2 - Z_{(k-1)i}^2 + Z_k^2 \end{vmatrix} \quad (3.15)$$

when $k \geq 4$.

Equation 3.12 can be solved in the sense of LSE minimization.

3.1.2 Time Difference of Arrival (TDOA)

TDOA is also known as the *hyperbolic positioning* technique. This method utilizes the same ranging procedures and results as does TOA. TDOA is based on estimating the difference in the arrival time of the signal between the synchronized reference nodes[1]. The position of node N_i is thus determined by assessing the difference between the time of arrival from the k reference nodes and N_i . It is assumed that the k reference nodes share a common time reference and that N_i is delayed with a time δ in respect to this. This delay is removed by subtraction between the time of arrival from different reference nodes. This is shown in the following equation:

$$D_{ni} - D_{(n-1)i} = c(\tau_{ni} + \delta) - c(\tau_{(n-1)i} + \delta) = c(\tau_{ni} - \tau_{(n-1)i}) \quad (3.16)$$

The position of Ni in a two-dimensional space is found similarly as in the TOA technique with a difference that instead of spheres, the intersection of hyperboloids gives the wanted position. This can be described by the following equation:

$$\left\{ \begin{array}{l} \sqrt{(X_2 - X_i)^2 + (Y_2 - Y_i)^2} - \sqrt{(X_1 - X_i)^2 + (Y_1 - Y_i)^2} \\ \sqrt{(X_3 - X_i)^2 + (Y_3 - Y_i)^2} - \sqrt{(X_2 - X_i)^2 + (Y_2 - Y_i)^2} \\ \vdots \\ \sqrt{(X_k - X_i)^2 + (Y_k - Y_i)^2} - \sqrt{(X_{k-1} - X_i)^2 + (Y_{k-1} - Y_i)^2} \end{array} \right\} = \left\{ \begin{array}{l} D_{2i} - D_{1i} \\ D_{3i} - D_{2i} \\ \vdots \\ D_{ki} - D_{(k-1)i} \end{array} \right\} \quad (3.17)$$

for $k \geq 3$.

When calculations are made in a three-dimensional space a minimum of four reference nodes is needed, as opposed to three in the case of two-dimensional positioning. This will not be taken into account in the simulations that are presented in the following chapters since they are done in a two-dimensional space. The positioning solution in a three-dimensional space can be found by taking into account and inserting the Z coordinate in equation 3.17.

As previously mentioned an accurate common time reference between the reference nodes is required. This does not apply to the relation between reference nodes and the target node. LSE is used in TDOA as well in order to reduce the ranging error.

3.1.3 Received Signal Strength (RSS)

An additional way of calculating the distance between two nodes (achieve ranging) is by applying the Received Signal Strength method [16]. The distance is derived by measuring the power and thus the attenuation of the received signal at a receiver node. In order to determine the two-dimensional location of a given node in a sensor network it is necessary to have at least three reference nodes, as is the case in TOA. One important aspect of achieving accurate ranging with RSS is that the method is very sensitive to estima-

tion of the characteristics of the channel. An accurate channel propagation model is necessary to achieve satisfactory results. This obviously reduces the accuracy of the RSS method in case of terminal mobility and channel variations.

In the case of RSS, the lower limit for a distance estimate \hat{d} achieved by the signal strength measurements is given by the Cramer-Rao lower bound, which in this case can be expressed by the following inequality [2]:

$$\sqrt{Var(\hat{d})} \geq \frac{\ln 10}{10} \frac{\sigma_{sh}}{n_p} d \quad (3.18)$$

Looking at the parameters that make up Equation 3.18, d is the distance between the two nodes, n_p is the path loss factor and σ_{sh} is the standard deviation of the zero mean Gaussian random variable representing the log-normal channel shadowing effect. From Equation 3.18 one can observe that the best achievable limit can be achieved by adapting the channel parameters and the distance between the two nodes. This is interesting in the sense that it shows that unique characteristics of a UWB signal, mainly the large bandwidth, are not exploited when RSS is applied [2]. The large bandwidth has no positive effect in the sense of increasing the achievable accuracy. This makes the RSS method less attractive in comparison to the time-delay methods discussed earlier, which offer an increased accuracy.

3.1.4 Angle of Arrival (AOA)

The AOA positioning technique is based on measuring of angles of the target node as seen from the reference nodes. This is done by applying antenna arrays. The position of the target node in a two-dimensional space is found by by measuring the angles of the straight line connecting the target node with the reference nodes.

The AOA method is not well suited to UWB positioning. Use of antenna arrays is impractical when small and cheap sensors are of interest. The increased system cost introduced by the arrays directly contradicts the main advantage of UWB radio which allows low-cost transmitters due to a large bandwidth. The large bandwidth of UWB signals creates additional problems regarding angle estimation. A large bandwidth implies a large number of possible paths from reference nodes to a target node. This leads to significant

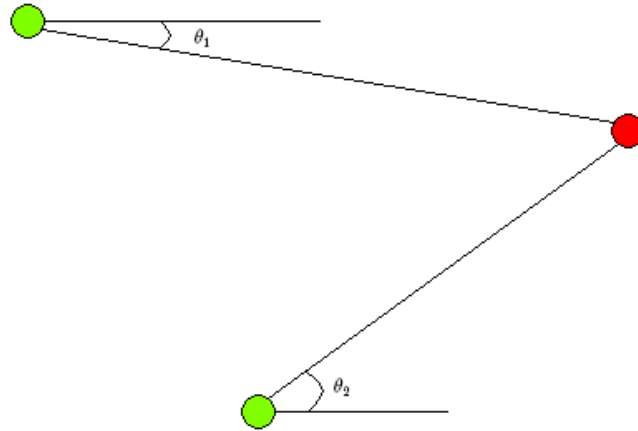


Figure 3.5: AOA positioning. The green nodes are the reference nodes.

challenges in angle estimation due to multipath and scattering from objects in the environment[2].

3.2 Comparison of the positioning techniques from the viewpoint of a UWB system

A description of the four common positioning techniques has been given in the previous sections of this chapter. Comparing the methods with each other gives a good indication on which are worth looking more into. AOA holds little interest from an UWB point of view because of the practical implementation. The necessary antenna arrays would be too unpracticle to implement while maintaining the low-cost demands of sensors. This has been confirmed by a comparative study [17] between AOA and TOA at the Université Catholique de Louvain. In that study CRB of the AOA is derived and compared with that of the time of arrival methods for UWB signals with spectral occupation that fulfills the FCC emission mask. The results show that for practical numbers of antenna arrays TOA always outperforms AOA. The accuracy of AOA is however still very good, although the technique is less effective for typical UWB signals experiencing strong scattering.

When comparing RSS with TOA based techniques it is again necessary to take into account the fact that RSS can not utilize the main advantage of UWB signals. The large bandwidth can not be exploited in the same way as with TOA techniques. Although it is easier to measure SS than TOA, the received ranging information is very coarse compared to the latter. A performance comparison of RSS and TOA has been done at the Worcester Polytechnic Institute[18]. The results showed that the TOA and RSS techniques are suited for 500MHz and 25 MHz systems respectively. This underlines the conclusion that TOA exploits the larger bandwidth of UWB signals, while RSS is more suited for narrowband signals.

The two time based techniques, TOA and TDOA have been found to be the most suitable for UWB positioning. Unlike RSS, the accuracy of a time based approach can be improved by increasing the SNR or the effective signal bandwidth. The large bandwidth of UWB signals allows extremely accurate location estimates. This high achievable accuracy of TOA is affected by clock synchronization between the nodes. Clock jitter is therefore an important factor to consider when evaluating the accuracy of a UWB positioning system. One way of dealing with this problem is by synchronizing the transmitted pulses by a delay-lock-loop (DLL) as presented in [19].

The difference between TOA and TDOA lies in synchronization between the nodes. There might not be synchronization between a given node and a reference node, but if synchronization exists between the reference nodes, then TDOA is a viable solution [2]. As described in the TDOA chapter, the difference in the arrival time between two signals from a target node to two reference nodes can be estimated and used to calculate the position of the target node. A third reference node is needed for complete localization in a two-dimensional plane.

Chapter 4

Simulations, results and discussions

A description of the main positioning methods and their adaptability to UWB technology has been given in Chapter 3. The conclusion reached is that the TDOA method is the most suited to positioning via UWB signals. In order to test the solution proposed in 3.1.2 a series of simulations will be presented in this chapter. Variables such as the number of, position of, and distance between nodes/sensors, available power to each node and sampling frequency will be assessed and their effects on the positioning results will be presented.

According to indications from WesternGeco, the sensors in a network are positioned as shown in figure 4.1.

The distance between the sensors varies from one up to fifteen meters. The network presented above can however be broken down into a nucleus consisting of seven nodes. The distance between neighbouring nodes is in this case the same. The simulations in this chapter will be based on this nucleus of seven nodes since this is more efficient than simulating an entire network. The constellation of the nucleus is shown in figure 4.2.

4.1 Description of the simulation process

Before presenting the simulation results it is necessary to give a description of the simulation process. A thorough description of each file used in the

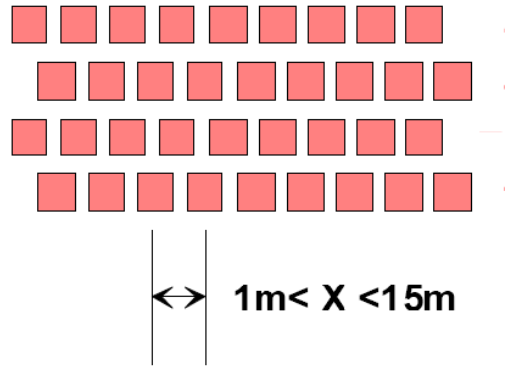


Figure 4.1: The sensor network imagined by WesternGeco

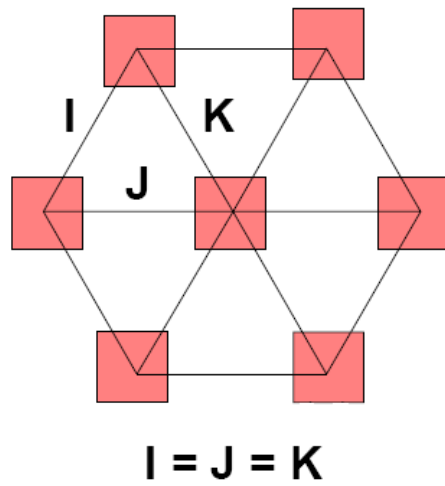


Figure 4.2: The nucleus consisting of seven nodes

simulation is given in the Appendix along with the Matlab codes. The short description given here is merely meant to ease the understanding of the results presented in the following sections.

The nodes of the network that is to be simulated are positioned in the pattern described in Figure 4.2. In order to simulate the positioning scheme involving these nodes it is necessary to establish a UWB-based network from scratch. Each of the nodes needs to be able to transmit and receive UWB signals. In addition to transmitters and receivers, a channel model will have to be simulated in order to achieve as realistic results as possible. A positioning scheme can then be implemented to test the accuracy under satisfactory conditions.

The simulation of the UWB network is based on a physical layer where PPM modulation is used in addition to TH, as described in section 2.1.1, in order to allow multiple access. The channel model is based on an indoor multipath UWB model proposed by the IEEE 802-15-SG3a committee. This model will be further described shortly. WesternGeco is a company that uses sensor technology in its seismic outdoors operations. The reason for choosing the mentioned indoor model for this simulation is that it is a well documented model that is also used in most other IR-UWB simulations. The author has not been able to track down a satisfactory outdoor UWB channel model. This is largely due to the fact that an absolute majority of the available literature on the subject is based on indoor experiments. The receiver is a RAKE receiver 2.3 that exploits the reflections of the signal and thus makes a better detection than a regular correlation-based receiver. An SRAKE with five branches has been selected for these simulations as it gives a satisfactory signal quality while not exceeding the possibilities of a realistic sensor design. The average antenna noise power at the receiver is white and Gaussian and is set at -83dBm in all simulations. This is a realistic estimate according to [5]. Perfect synchronization between the transmitter and receiver is assumed. This is done as to reduce the complexity of the code. A possible way to achieve synchronization could have been to incorporate a synchronization sequence at the head of each information package transmitted. This sequence would be known to all participants of the network and a correlation filter matched to the sequence could be used [3]. The implementation of the code is done in MATLAB. Part of the code is based on examples given in [3]. Some of the files are used unedited, while some have been modified to fit in the whole scheme of the simulation. Information regarding the degree of modification within each file will be listed in the appendix.

It is also important to note that the exact values of the results of the calculations are not necessarily as important as the tendencies that can be clearly seen by changing variables like the power level at the transmitter. Each value of the average positioning error, ErrNx, has been found on a basis of five independent calculations. This is a small number that has been chosen out of necessity since calculations of tens or hundreds of independent examples for each case would be extremely time consuming and would surpass the ability of the computer used. The calculated values of ErrNx and the values of corresponding parameters are thus more strong pointers and indicators.

4.1.1 The Channel model

The channel model applied in the simulation is the IEEE 802.15.SG3 channel model. The information presented in this section is gathered from [3] and [5]. This channel model was first proposed by the IEEE 802.15.SG3 committee in 1972 and later formalized by Saleh and Valenzuela in 1987. The goal was to select the best indoor channel model for IR-UWB signals based on multipath fading. The model is based on the observation that the multipath contributions of a single pulse arrive at the receiver in clusters. The time of arrival of these clusters is modeled to be Poisson distributed with a rate Λ . The multipath contributions within each cluster are also thought to be Poisson distributed with a rate λ . The channel impulse response can be expressed as follows:

$$h(t) = X \sum_{n=1}^N \sum_{k=1}^{K(n)} \alpha_{nk} \delta(t - T_n - \tau_{nk}) \quad (4.1)$$

where X is a log-normal random variable representing the amplitude gain of the channel, N is the number of observed clusters, $K(n)$ is the number of multipath contributions received within the n -th cluster, α_{nk} is the coefficient of the k -th multipath contribution of the n -th cluster, T_n is the time of arrival of the n -th cluster and τ_{nk} is the delay of the k -th multipath contribution within the n -th cluster.

The channel coefficient is given by:

$$\alpha_{nk} = p_{nk} \beta_{nk} \quad (4.2)$$

where p_{nk} is ± 1 with equal probability and β_{nk} is the log-normal distributed channel coefficient of multipath contribution k belonging to cluster n . The channel model has parameters defined for four different scenarios. These are:

- LOS (0-4 m)
- NLOS (0-4 m)
- NLOS (4-10 m)
- Extreme NLOS

The simulations have been performed according to these scenarios but with some notable differences. These will be described shortly. This is done in order to achieve an as realistic scenario as possible for the positioning scheme. The parameters in the original case are defined for LOS distances up to four meters and NLOS distances up to ten meters. In the following simulations and the subsequent MATLAB codes, it is assumed that the channel parameters for LOS are the same for distances larger than 4 meters while the same parameters also apply for distances above 10 m as for distances 4-10 m for the NLOS scenario. Even though they are a necessary part of the code, the cases involving NLOS will not be considered. The reason for this is that the IEEE 802.15.SG3 channel model is an indoor model. It is based on measurements of the multipath cluster distribution in an indoor office environment[20]. In these kinds of environments the effects of NLOS, because of many objects that might be in the way, are much stronger than in an outdoor environment. Indoor LOS will thus provide a more realistic platform for the case considered in this report. The channel parameters are listed in the appendix.

One of the possible scenarios described above will be selected according to the distance d between the nodes and the LOS/NLOS situation. A impulse response $h(t)$ for the channel will then be generated and a convolution between this $h(t)$ and the transmitted signal will be performed as to simulate the signal at the receiver.

$P(\text{dBm})$	$f_c(\text{GHz})$	$d(\text{m})$	$ErrNx(\text{m})$
-20	22	7	117.2594
-15	22	7	89.8327
-10	22	7	4.4505
-5	22	7	0
-10	44	7	0

Table 4.1: Effects of power variation on the positioning accuracy.

4.2 Simulation scenarios

The simulations in this chapter will test the TDOA positioning method under different conditions. The accuracy of the positioning scheme will be evaluated on the basis of the presented results and a best possible solution will be discussed.

4.2.1 Power and sampling frequency variations

The effects of the amount of available power to the sensors in a network will be inspected in this section. As discussed in section 2, a signal that perfectly fills the available 3,1GHz-10,6GHz bandwidth gives a maximum transmission power of 0.55mW (-2.6dBm) when integration over the FCC mask is performed. It is however unrealistic to achieve this power level without exceeding the emission mask. The reason is that the pulse shaping and dispersing of the pulses in the time domain would have to be perfect and thus strictly non-overlapping while at the same time filling the emission mask completely in order to achieve this. The necessity of non overlapping pulses is taken into account when selecting a sampling frequency f_c . As discussed in chapter 2.4, the sampling frequency must be at least 21.2 GHz as to avoid aliasing. The accuracy of the positioning scheme when different power levels and sampling frequencies are applied are presented in table 4.1. The distance between the nodes has been fixed to 7 m in order to examine the effects of power and frequency variation under constant conditions. The main emphasis is on power variation since power consumption is the most interesting aspect of UWB technology.

It can be clearly seen from Table 4.1 that the average positioning error, $ErrNx$, decreases drastically when the available power level is increased. The reason is of course that a stronger emitted signal is, after being affected by

the channel, relatively larger than the noise at the receiver when compared to a signal with lower power. The effects of these power variations for two random measurements are shown in Figures 4.3 and 4.4 where TN is the actual position of the target node, while PosNx is the position estimated by the positioning scheme.

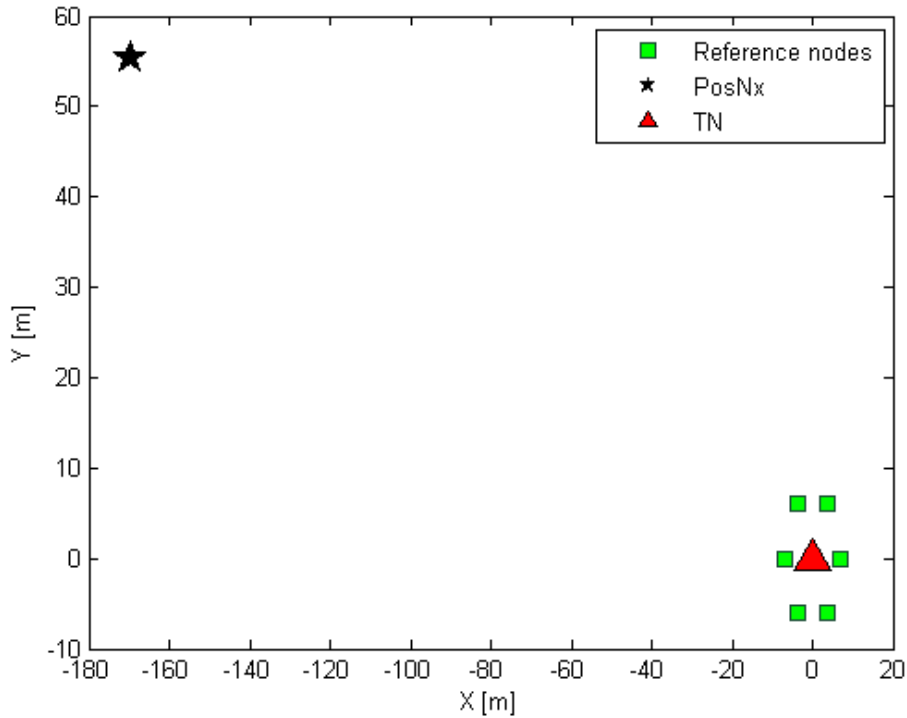


Figure 4.3: The result of the positioning scheme for a distance of 7 m and an available power of -20 dBm

With table 4.1 still in mind, it can be observed that an average positioning error of 0 for a distance of 7 m between the nodes can be achieved in two ways. These are by either increasing the power level to -5 dBm for a minimum sampling frequency of 22 GHz, or setting the power level at -10 dBm while increasing the sampling frequency to 44 GHz. Increased sampling frequency leads to increased representation of the transmitted signal and thus better positioning results. Both methods reduce ErrNx and the choice of which one to increase can be seen as a tradeoff in sensor design.

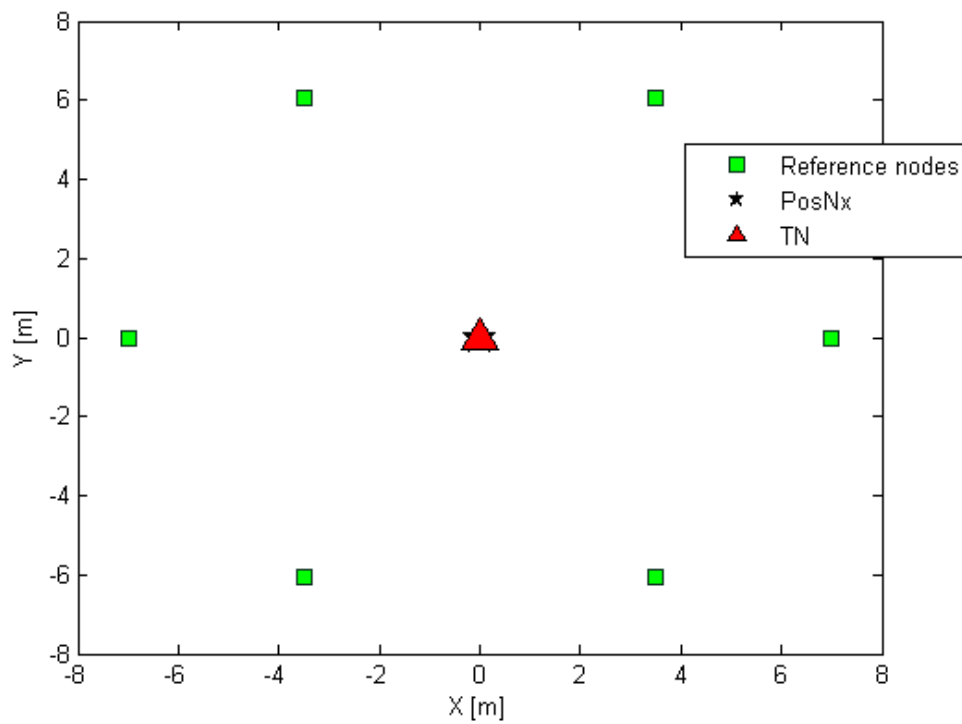


Figure 4.4: The result of the positioning scheme for a distance of 7 m and an available power of -5 dBm

$P(dBm)$	$fc(GHz)$	$d(m)$	$ErrNx(m)$
-10	22	4	4.9343e-017
-10	22	8	30.8066
-10	22	15	49.2898
-10	55	15	18.3922
-5	55	15	0

Table 4.2: Effects of distance variation on the positioning accuracy.

4.2.2 Distance between the nodes

The impact of the distance between the sensors in a UWB network is assessed in this chapter. The sensors are placed as shown in Figure 4.2 with equal distances between neighbours. Increasing this distance enables the nucleus of seven sensors, and thus the total network shown in Figure 4.1, to cover a larger geographical area. WesternGeco indicates a maximum distance between neighbouring sensors to be at 15 m. Table 4.2 shows the impact on the average estimation error that occurs when the distance d is gradually increased.

It can be seen that the average error increases dramatically with the increased distance. This is to be expected as the signal is further attenuated for every additional bit of distance it has to cover over the channel on its way from the transmitter to the receiver. The more the signal gets attenuated, the weaker it is compared to the noise at the receiver upon arrival. This SNR has a direct influence on the accuracy of the positioning scheme as the relatively large noise level distorts the ranging measurements which are used in the LSE.

Table 4.2 further shows that increasing the power and/or the sampling frequency of the output signal can improve the ranging accuracy and thus the positioning results. The results in table 4.3 suggest power levels combined with certain sampling frequencies that provide positioning results with small and acceptable average positioning errors. These results have been achieved by testing different combinations of fc and P .

$P(\text{dBm})$	$f_c(\text{GHz})$	$d(\text{m})$	$ErrNx(\text{m})$
-10	22	4	4.9343e-017
-10	55	8	0.0104
-7	55	12	8.4022e-4
-5	55	15	8.0147e-4

Table 4.3: Optimal distance between the nodes.

4.2.3 Position of target node

This chapter addresses the case when the target node is not in the middle of the nucleus presented in Figure 4.2. This is necessary in order to achieve positioning of the sensors that, due to their position on the edges of the overall network, can not be placed in the middle of the nucleus. The network indicated by WesternGeco is built on the principle of equal distance between neighbouring sensors. It can be observed from Figure 4.5 which sensors can be positioned by being placed in the middle of the nucleus. These sensors are colored green. This can be done by constant redefining of the target node in the simulation and subsequently selecting the surrounding sensors as reference nodes. The other sensors, the pink ones in Figure 4.5, can not be placed in the middle of any nucleus consisting of 7 nodes.

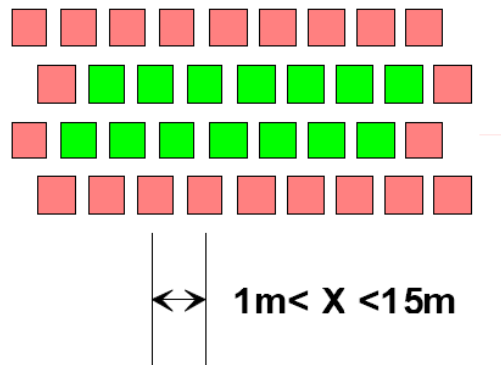


Figure 4.5: Sensors that can be positioned as centres of a nucleus

Results achieved by simply defining the target node to the edge of the nucleus and using the six remaining nodes in the network as reference nodes are shown in table 4.4.

$P(dBm)$	$f_c(GHz)$	$d(m)$	Reference nodes	$ErrNx(m)$
-5	55	15	6	18.1950
-10	44	7	6	22.2975

Table 4.4: Positioning error when the target node is set to the edge of the nucleus.

$P(dBm)$	$f_c(GHz)$	$d(m)$	Reference nodes	$ErrNx(m)$
-5	55	15	3	12.4000e-4
-10	44	7	3	0

Table 4.5: Positioning error when the nodes farthest off are discarded and only three reference nodes are used.

Comparing the values in table 4.4 with the corresponding presented in tables 4.1 and 4.3 one can see that the average positioning error is greatly increased. This is due to the additional distance the signal must travel over the channel compared to the case when the target node is in the center of the nucleus. Instead of an equal distance between each sensor, the signal must now cover a significantly larger distance in order to reach three nodes that are farthest off. In fact, the largest distance to be covered is twice the size of the distance between the sensors when the target node is placed in the middle of the nucleus. The problem and the error introduced with it are illustrated by Figure 4.6. The case presented is for $P=-5dBm$, $d=15m$ and $f_c=55GHz$.

As described in chapters 3.1.1 and 3.1.2 it is necessary to have a minimum of three reference nodes in order to find the position of a target node in a two-dimensional space. This implies that three nodes may be enough to accurately position a target node. According to this theory, it was decided by the author of this report to discard the three reference nodes farthest off the target node and leave the three nearest sensors as reference nodes. The signal from the discarded nodes will be severely attenuated because of the long distance it must travel and will thus provide inaccurate ranging measurements which in the end will distort the position estimation. The author decided to break down the nucleus, which has so far been the basis of all simulations, into a network consisting of four nodes where the three reference nodes are equally distanced from the target node. This was done in order to try to deal with the problem described above. The situation is illustrated in Figure 4.7 and the effect on the average positioning error is presented in table 4.5.

By comparing $ErrNx$ in tables 4.4 and 4.5 it can be concluded that discarding

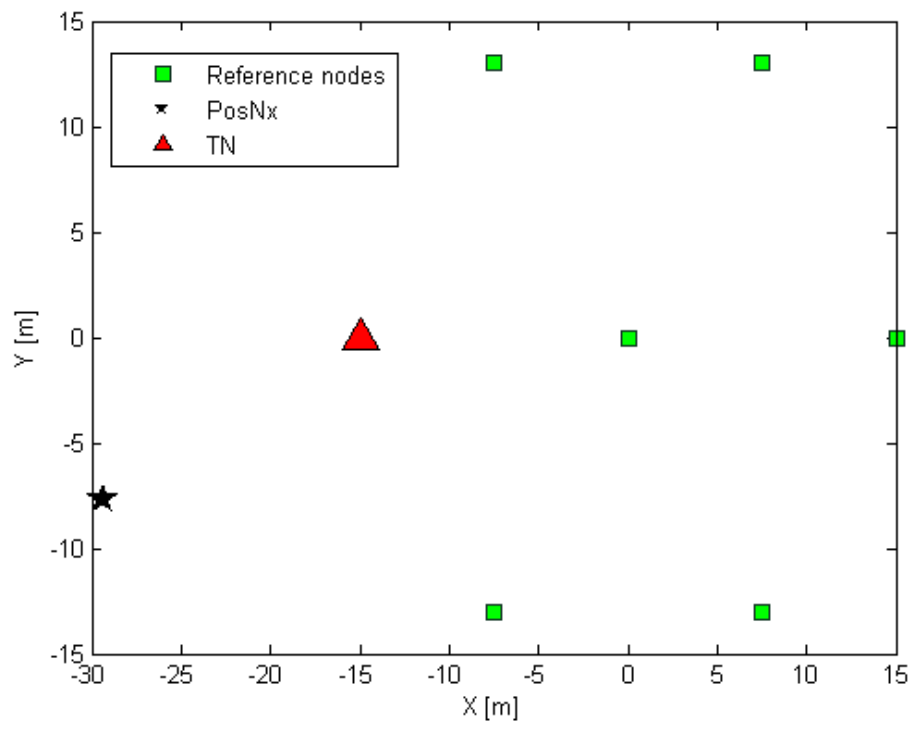


Figure 4.6: The result of the positioning scheme when the target node is at the edge of the nucleus.

$P(\text{dBm})$	$f_c(\text{GHz})$	$d(\text{m})$	Reference nodes	$ErrNx(\text{m})$
-5	55	15	4	0
-10	44	7	4	0

Table 4.6: Positioning results when four reference nodes are used.

the reference nodes that were farther away the target node than the fixed distance d was the right move. The severely attenuated signals from these nodes are in this way prevented to influence the positioning scheme by supplying corrupted ranging information. Four of the remaining sensors in the network can be positioned in this way by using only three reference nodes. These are marked by the purple color in Figure 4.8. The three nearest nodes are of course selected as reference nodes.

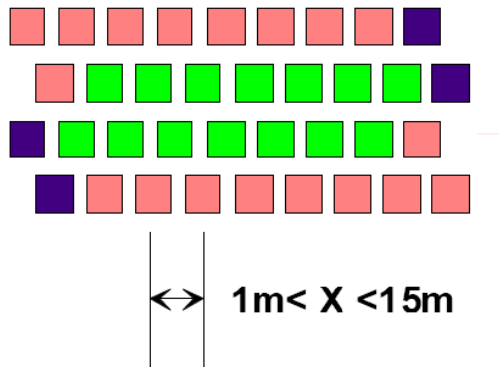


Figure 4.8: Sensors at the edges that can be found by using only three reference nodes.

The sensors in the top and bottom row respectively can be positioned by using the four nearest sensors as reference nodes. In a similar way as in the example with three reference nodes, the two sensors that are not available are discarded from the equation. The results from this positioning scheme are presented in Figure 4.9 and table 4.6. Comparison of tables 4.6 and 4.5 shows increased positioning accuracy in the case of $P = -5\text{dBm}$, $f_c = 55\text{GHz}$ and $d = 15\text{m}$ when four reference nodes are used. This supports the theoretical assumptions presented in chapter 3 that an increased number of reference nodes increases the positioning accuracy.

Figure 4.10 shows the network after all the proposed positioning scenarios have been realized. The green colored sensors can be positioned by the use of

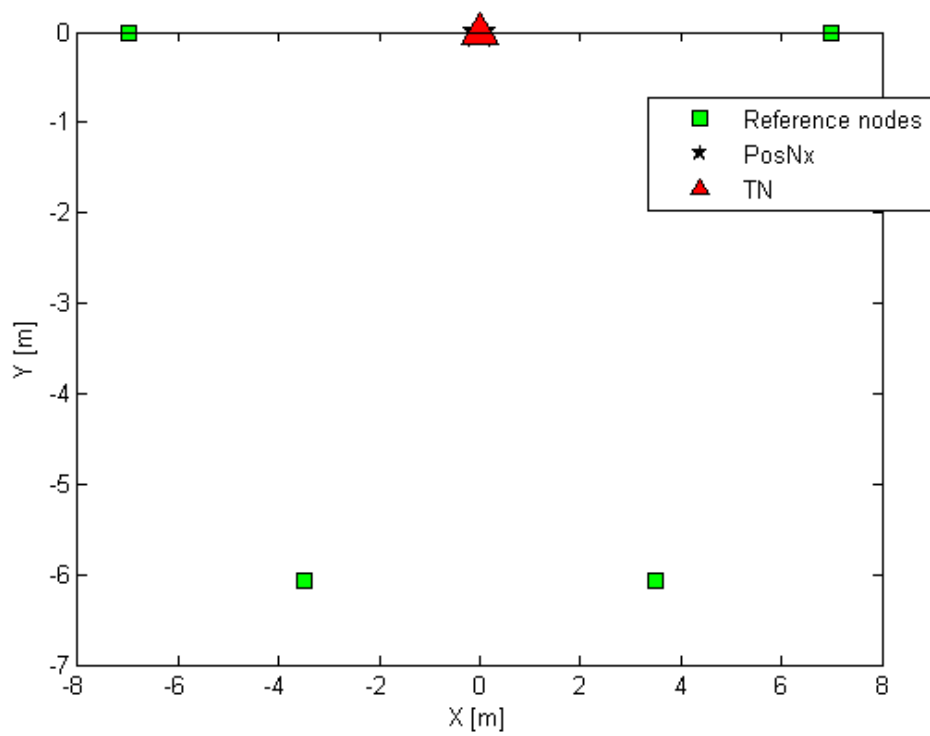


Figure 4.9: Positioning scheme when two reference nodes are discarded.

$P(dBm)$	$f_c(GHz)$	$d(m)$	Reference nodes	$ErrNx(m)$
-5	55	15	3	7.1091
-10	44	7	3	8.1600

Table 4.7: Positioning results when the nearest non-neighbouring sensor is selected as the third reference node.

both the original nucleus with six reference nodes positioned around a target node in the center, and the solution with only three reference nodes. The dark and light purple colored sensors can be positioned by the use of four and five reference nodes respectively. This is done by adapting the nucleus in such a way that reference nodes are discarded as to fit the requirements of the target node.

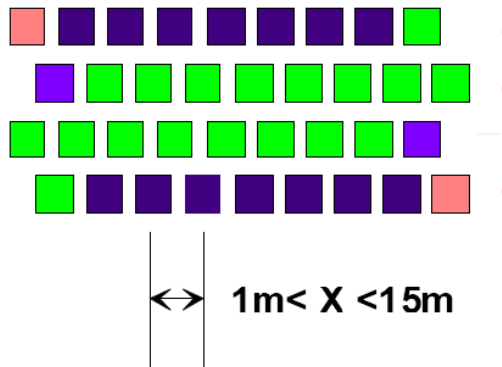


Figure 4.10: Sensors that can be positioned by the use of the methods described thus far.

The only two sensors that are yet to be positioned are the two shown in pink on Figure 4.10. These sensors are placed on the two diagonal edges of the network. As can be seen from the figure, these sensors only have two neighbours which can be used as reference nodes in a positioning scheme. In two-dimensional positioning, a minimum of three reference nodes is needed. Selecting the nearest non-neighbouring sensor as the third reference node is tested and the results are presented in table 4.7. An illustration is provided in Figure 4.11. As expected, an positioning error is introduced because of the extra distance the transmitted signal must travel from the reference node farthest off when compared to the neighbouring nodes.

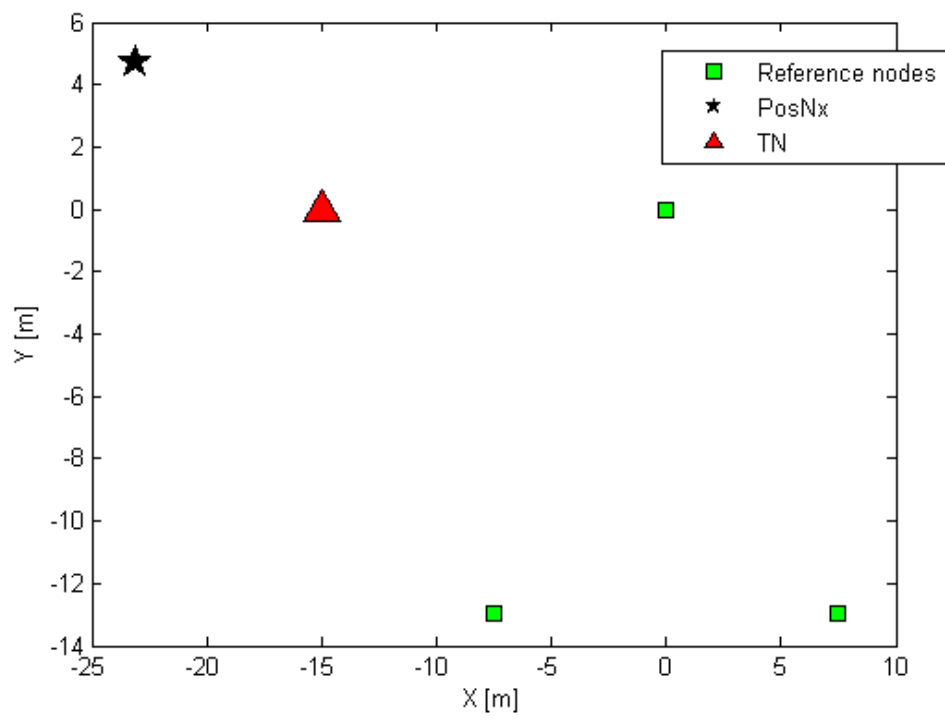


Figure 4.11: The third reference node is an non-neighbouring sensor.

In order to counter this problem and achieve positioning for the two mentioned sensors, the author of this report proposes to expand the network with two additional sensors. These can be placed as proposed in Figure 4.12 where the sensors to be added are colored red. By placing the two sensors as proposed it is possible to select three neighbouring nodes as reference nodes for every sensor in the network. Positioning by the use of at least three reference nodes can thus be achieved in each case.

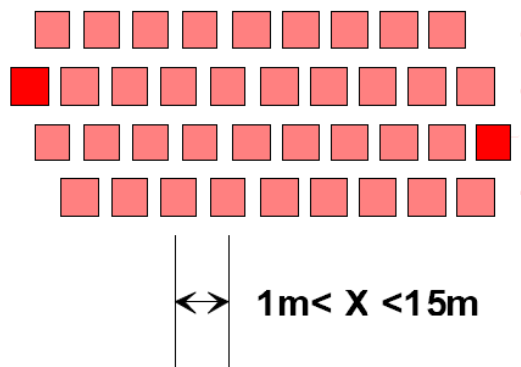


Figure 4.12: Proposed positions for the two sensors to be added.

Chapter 5

Conclusions

The TDOA positioning scheme has been tested under realistic conditions in this chapter. Several conclusions can be drawn from the presented results. The power level available at the transmitter is crucial to the accuracy of the positioning scheme. This was no surprise since UWB operates at low power levels and each increase in power availability is welcome. The sampling frequency can also be used to increase the accuracy of the positioning scheme by achieving higher representation of the transmitted signal. These two factors are key to determining the capacity and ability of the positioning scheme.

WesternGeco have indicated that the distance between sensors in a network varies between 1 m and 15 m. The simulation results show that it is to a large extent possible to use the proposed TDOA solution in order to implement positioning between the sensors. The maximum transmitter power allowed is -2.6 dBm. This level is as previously mentioned unrealistic to achieve. As can be seen from the tables listed earlier in this chapter, a power level of -10 dBm has been frequently chosen. The reason is that this level is sufficiently lower than the maximum allowed for it to be quite realistic to implement in real life. As can be seen from table 4.3 an accuracy of approximately 1 cm can be achieved by adopting a power level of -10 dBm and a sampling frequency of 55 GHz for a distance of 8 m between the sensors. The relatively high frequency has led to choosing higher power levels for simulations above 8 m. Again referring to the results presented in table 4.3, it can be seen that low average positioning errors can be achieved for distances of 12 and 15 meters with power levels -7.5 dBm and -5 dBm respectively. The sampling frequency is in both cases set at 55 GHz.

These results show that it is possible to achieve accurate positioning using

the TDOA scheme for distances up to 15 meters without exceeding the -2.6 dBm power limit. In some cases it is however necessary to come quite close to the limit in order to reach these goals. It may be quite challenging to implement a power level of -5 dBm, and also -7.5 dBm to a lesser extent, in real life solutions without exceeding the emission mask presented by the FCC. The whole process of selecting the power level and sampling frequency is based on making trade-offs in order to reduce receiver and transmitter complexity.

A conclusion can be reached that for distances up to 8 m one can reach satisfactory positioning results under reasonable power levels and sampling frequencies. For distances larger than 8 meters it is still possible to achieve accurate positioning. It is however necessary to operate close to existing power and frequency limitations.

Another problem that has been addressed in the simulations is the case of positioning the sensors that are on the edge of the network. These can not be viewed as the center node of a nucleus. The problems have been presented and the solution is to adapt the nucleus so as to use as many neighbouring sensors as possible for reference tasks. The overall network should, when implemented, be able to decide whether the target node is on the edge of the network and adapt the positioning scheme as needed. It is also shown that an increased number of reference nodes provides more accurate positioning results. This is however the case only when the neighbouring sensors are used as reference nodes. Choosing sensors that are not neighbours only increases the average positioning error by providing corrupted ranging information. It is also important to note that in order to enable at least three neighbouring reference nodes to any given sensor in the network, it is necessary to expand the network proposed by WesternGeco by two additional sensors. These are to be placed as proposed in Figure 4.12

To sum it all up, a realization of the network imagined by WesternGeco should be possible for distances up to 15 meters by applying a transmitter power of up to -5 dBm and a sampling frequency of 55 GHz. Positioning with shorter distances between the nodes may be achieved by lower transmitter power and sampling frequencies. All networks should have the ability to distinguish whether the target node is on the edge of the network or not, and act accordingly.

5.1 Future work

Even though some aspects of positioning and UWB have been covered in this report, there are still many things that might be worth looking further into. This report presents four positioning schemes and makes a comparison between them with an outlook on UWB-adaptability. One of the methods, TDOA, is selected as the most promising and tested. There are however so-called hybrid solutions that might prove to offer some interesting benefits. One such is the TDOA/AOA hybrid using extended Kalman filters presented in [21]. Biased or unbiased Kalman filters are used for estimation of the TOA (ranges). The use of this and possible other hybrid methods can be investigated with a view of surpassing the TDOA positioning scheme presented in this report.

The simulations in this work have been based on the IEEE 802.15.SG3 indoor channel model. This provides a relatively realistic environment in which to propagate the signals between the transmitter and receiver. WesternGeco uses its sensor network mostly for outdoor seismic operations. For these purposes it would be even more optimal to test the method presented in this report under conditions that emulate an outdoor environment. A continuation on the work presented here can be related to implementing the positioning scheme with an outdoor channel model for UWB signals. Such a channel model has proved to be hard to come by so a solution may be to try to modify an existing indoor channel model.

The results presented in this report give more of an indication rather than definite values of power levels and sampling frequencies that are suited for positioning with certain distances between the sensors. The reason is that each average positioning error value has been calculated out of only five calculations/measurements. This is because more definite calculations would require perhaps a hundred independent simulations for each case. This was not feasible in this project mainly due to the lack of computer power, but also because of time aspect. A verification and further investigation into power levels and sampling frequency values, and the combination of these in order to achieve optimal positioning can be seen as future work.

Finally, an implementation of a large-scale network consisting of multiple nucleuses can be tested. A built-in scheme for selecting an optimal number of nodes as references for positioning at the edges can be added in order to

evaluate the performance under even more realistic conditions.

Bibliography

- [1] Jun Xu, Maode Ma, and Choi Look Law. Position estimation using uwb tdoa measurements. *Ultra-Wideband, The 2006 IEEE 2006 International Conference on*, pages 605–610, Sept. 2006.
- [2] Sinan Gezici, Zhi Tian, Georgios B. Giannakis, Hisashi Kobayashi, Andreas F. Molisch, Vincent Poor, and Zafer Sahinoglu. Localization via ultra-wideband radios. *IEEE Signal Processing Magazine*, pages 70–84, December 2005.
- [3] Maria-Gabriella Di Benedetto and Guerino Giancola. *Understanding Ultra Wide Band. Radio Fundamentals*. Prentice Hall PTR, 2004.
- [4] Xuemin (Sherman) Shen, Weihua Zhuang, Hai Jiang, and Jun Cai. Medium access control in ultra-wideband wireless networks. *IEEE Transactions On Vehicular Technology, VOL. 54, NO. 5*, pages 1663–1677, September 2005.
- [5] Nathaniel J. August, Dr. Dong S. Ha, Dr. James R. Armstrong, Dr. Thurman E. Lockhart, Dr. Jeffrey H. Reed, and Dr. Joseph G. Tront. Medium access control in impulse-based ultra wideband ad hoc and sensor networks. *PHD, Virginia Polytechnic Institute and State University*, pages 1–226, 2002.
- [6] Xuemin (Sherman) Shen, Weihua Zhuang, Hai Jiang, and Jun Cai. Medium access control in ultra-wideband wireless networks. *Vehicular Technology, IEEE Transactions on*, pages 1663– 1677, September 2005.
- [7] Dongsong Zeng, Annamalai Annamalai Jr., , and Amir I. Zaghoul. Pulse shaping filter design in uwb system. *Ultra Wideband Systems and Technologies, 2003 IEEE Conference on*, 16-19 Nov. 2003.

-
- [8] Arne Svensson. Introduction to and some results on ds-uwband, multiband uwband, and multiband ofdm. *Chalmers, Department of Signals and Systems*, 2004.
- [9] Muhammad Gufran Khan, Jörgen Nordberg, Abbas Mohammed, and Ingvar Claesson. Performance evaluation of rake receiver for uwband systems using measured channels in industrial environments. *Blekinge Institute of Technology*.
- [10] Andrea Goldsmith. *Wireless Communications*. Cambridge University Press, 2005.
- [11] Leonard E. Miller. Why uwband? a review of ultrawideband technology. *National Institute of Standards and Technology, Gaithersburg, Maryland*, April 2003.
- [12] Jian Zhang. Short-range high-speed ultra wideband communications. *PHD, The Australian National University*, pages 1–165, September 2004.
- [13] Simon Haykin. *Communication Systems 4th Edition*. John Wiley & Sons, Inc., 2001.
- [14] Zhang Xinyu, Sha Xuejun, and Sheng Rennong. Performance of ranging and positioning models with impulse uwband. *Wireless Communications, Networking and Mobile Computing, 2006. WiCOM 2006. International Conference on*, 22-24 Sept. 2006.
- [15] Rashid A. Saeed, Sabira Khatun, Brohanuddin Mohd., and Mohd. A. Khazani. Performance of ultra-wideband time-of-arrival estimation enhanced with synchronization scheme. *ECTI Transactions on electrical eng., electronics, and communicationc, VOL 4, No.1*, pages 78–84, February 2006.
- [16] Ahmad Hatami, Kaveh Pahlavan, Mohammad Heidari, and Ferit Akgul. On rss and toa based indoor geolocation - a comparative performance evaluation. *IEEE Wireless Communications and Networking Conference*, April 3.-6. 2006.
- [17] Achraf Mallat, J. Louveaux, and L. Vandendorpe. Uwband based positioning: Cramer rao bound for angle of arrival and comparison with time of arrival. *Communications and Vehicular Technology, 2006 Symposium on*, pages 65–68, 2007-03-19.
- [18] Ahmad Hatami and Kaveh Pahlavan. Performance comparison of rss and toa indoor geolocation based on uwband measurement of channel char-

-
- acteristics. *Personal, Indoor and Mobile Radio Communications, 2006 IEEE 17th International Symposium on*, pages 1–6, 2006-12-11.
- [19] Yuichiro Shimizu and Yukitoshi Sanada. Accuracy of relative distance measurement with ultra wideband system. *Ultra Wideband Systems and Technologies, 2003 IEEE Conference on*, pages 374– 378, 2004-03-03.
- [20] J. R. Foerster. Channel modeling sub-committee report final. *IEEE P802.15-02/368r5-SG3a*, 2002. IEEE P802.15 Working Group for WPAN.
- [21] Chi-Der Wann, Yi-Jing Yeh, and Chih-Sheng Hsueh. Hybrid tdoa/aoa indoor positioning and tracking using extended kalman filters. *Vehicular Technology Conference, 2006. VTC 2006-Spring. IEEE 63rd*, pages 1058–1062, 2006.

Appendix A

Appendix

A.1 IEEE 802.15.SG3 channel model parameters

Target Channel Characteristics ⁵	CM 1 ¹	CM 2 ²	CM 3 ³	CM 4 ⁴
Mean excess delay (nsec) (τ_m)	5.05	10.38	14.18	
RMS delay (nsec) (τ_{rms})	5.28	8.03	14.28	25
NP _{10dB}			35	
NP (85%)	24	36.1	61.54	
Model Parameters				
Λ - cluster arrival rate (1/nsec)	0.0233	0.4	0.0667	0.0667
λ - ray arrival rate (1/nsec)	2.5	0.5	2.1	2.1
Γ - cluster decay factor	7.1	5.5	14.00	24.00
γ - ray decay factor	4.3	6.7	7.9	12
σ_1 cluster fading s.d. (dB)	3.3941	3.3941	3.3941	3.3941
σ_2 ray fading s.d. (dB)	3.3941	3.3941	3.3941	3.3941
σ_x total shadowing s.d. (dB)	3	3	3	3
Model Characteristics ⁵				
Mean excess delay (nsec) (τ_m)	5.0	9.9	15.9	30.1
RMS delay (nsec) (τ_{rms})	5	8	15	25
NP _{10dB}	12.5	15.3	24.9	41.2
NP (85%)	20.8	33.9	64.7	123.3
Channel energy mean (dB)	-0.4	-0.5	0.0	0.3
Channel energy std (dB)	2.9	3.1	3.1	2.7
¹ LOS (0-4m). Channel measurements reported in [202].				
² NLOS (0-4m). Channel measurements reported in [202].				
³ NLOS (4-10m). Channel measurements reported in [202],[203].				
⁴ Extreme NLOS. 25 nsec RMS delay spread.				
⁵ These characteristics are based upon a 167 psec sampling time.				

Figure A.1: Parameters for the IEEE 802.15.SG3 channel model

A.2 MATLAB files

Files programmed entirely by the author and files from [3] that have in some way been altered by the author will be listed in this appendix. The files from [3] that have not been altered will only be attached to the report and not listed here.

A.2.1 *Posisjonering_hovedfil.m*

```
%This is the main file in the simulation process.
%The file determines the LSE solution to a positioning problem in a
%bidimensional space.
%It is based on file "cp1002_find_LSE_position" but significant
%changes have been made.
%
%The file no longer functions as a function, that is, all the necessary
%parameters are defined either in posisjonering_hovedfil.m itself or
%posisjonering.m
%
%
% The file generates the estimated position of
% the target node Nx and the error with respect to the
% exact position ErrNx
%
%
%Programmed by Luca De Nardis, edited by the author.
%

%Part of the original code by Luca De Neris
%function [PosNx, ErrNx] = cp1002_find_LSE_position(positions,
%ranges, Nx, Ref,sigma_2, G);

n=7                                %Distance between the nodes, described as I=J=K in
    %the report.
```

```

zeros(7,2)
positions(1,1)=0           %A matrix 'positions' is generated containing positions
positions(1,2)=0           %of the nodes placed as described in the report.
positions(2,1)=-n
positions(2,2)=0
positions(3,1)=-n/2
positions(3,2)=-sqrt(((n^2)-(n/2)^2))
positions(4,1)=n/2
positions(4,2)=-sqrt(((n^2)-(n/2)^2))
positions(5,1)=n
positions(5,2)=0
positions(6,1)=n/2
positions(6,2)=sqrt(((n^2)-(n/2)^2))
positions(7,1)=-n/2
positions(7,2)=sqrt(((n^2)-(n/2)^2))

zeros(7,7)
ranges=zeros(7,7)         %A matrix 'ranges' is generated containing the
ranges(1,1)=0             %distances between each pair of nodes.
ranges(1,2)=n
ranges(1,3)=n
ranges(1,4)=n
ranges(1,5)=n
ranges(1,6)=n
ranges(1,7)=n
ranges(2,1)=n
ranges(2,2)=0
ranges(2,3)=n
ranges(2,4)=sqrt((n+n/2)^2+((n^2)-(n/2)^2))
ranges(2,5)=2*n
ranges(2,6)=sqrt((n+n/2)^2+((n^2)-(n/2)^2))
ranges(2,7)=n
ranges(3,1)=n
ranges(3,2)=n
ranges(3,3)=0
ranges(3,4)=n
ranges(3,5)=sqrt((n+n/2)^2+((n^2)-(n/2)^2))
ranges(3,6)=2*n
ranges(3,7)=(2*sqrt(((n^2)-(n/2)^2)))
ranges(4,1)=n
ranges(4,2)=sqrt((n+n/2)^2+((n^2)-(n/2)^2))

```

```

ranges(4,3)=n
ranges(4,4)=0
ranges(4,5)=n
ranges(4,6)=(2*sqrt(((n^2)-(n/2)^2)))
ranges(4,7)=2*n
ranges(5,1)=n
ranges(5,2)=2*n
ranges(5,3)=sqrt((n+n/2)^2+((n^2)-(n/2)^2))
ranges(5,4)=n
ranges(5,5)=0
ranges(5,6)=n
ranges(5,7)=sqrt((n+n/2)^2+((n^2)-(n/2)^2))
ranges(6,1)=n
ranges(6,2)=sqrt((n+n/2)^2+((n^2)-(n/2)^2))
ranges(6,3)=2*n
ranges(6,4)=(2*sqrt(((n^2)-(n/2)^2)))
ranges(6,5)=n
ranges(6,6)=0
ranges(6,7)=n
ranges(7,1)=n
ranges(7,2)=n
ranges(7,3)=(2*sqrt(((n^2)-(n/2)^2)))
ranges(7,4)=2*n
ranges(7,5)=sqrt((n+n/2)^2+((n^2)-(n/2)^2))
ranges(7,6)=n
ranges(7,7)=0

Nx=1           %Selects the target node.
Ref=[2 3 4 5 6 7] %Selects the reference nodes
G=1

distanse=ranges(1,2:length(ranges(1,:))) %Estimates the REAL distance between
%the reference nodes ant the target node.
[estimert_avstand] = posisjoningering(distanse) %Uses the real distance
%'distanse' to find an
%estimate of the distance
%between the ref. nodes and
%the target node using the
%ranging methods in
%posisjoningering.m

```

```

%%%%%%%%%%%%%%%%%%%%%%%%%%%%%%%%%%%%%%%%%%%%%%%%%%%%%%%%%%%%%%%%%%%%%%%%
%Uses the LSE method to find the position of the target node based on the
%estimated distance to the reference nodes.
%%%%%%%%%%%%%%%%%%%%%%%%%%%%%%%%%%%%%%%%%%%%%%%%%%%%%%%%%%%%%%%%%%%%%%%%

%N = size(ranges,1);
%err_ranges = ranges + sqrt(sigma_2)*randn(N); The error added in the
%original code
err_ranges=zeros((length(Ref)+1),1);
err_ranges(2:(length(Ref)+1),1)=transpose(estimert_avstand); %the error
%added through 'posisjonering.m'
%by using 'estimert_avstand'

%%%%%%%%%%%%%%%%%%%%%%%%%%%%%%%%%%%%%%%%%%%%%%%%%%%%%%%%%%%%%%%%%%%%%%%%The rest of the code is unchanged by the author%%%%%%%%%%%%%%%%%%%%%%%%%%%%%%%%%%%%%%%%%%%%%%%%%%%%%%%%%%%%%%%%%%%%%%%%

% Defining the linear problem
% Matrix A
k = length(Ref);
for i=1:(k-1)
    A(i,1) = positions(Ref(i),1) - positions(Ref(k),1);
    A(i,2) = positions(Ref(i),2) - positions(Ref(k),2);
end
A=-2*A;
% Matrix b
b=zeros(2,1);
for i=1:(k-1)
    b(i) = err_ranges(Ref(i),Nx)^2 - ...
    err_ranges(Ref(k),Nx)^2 - positions(Ref(i),1)^2 + ...
    positions(Ref(k),1)^2 - positions(Ref(i),2)^2 + ...
    positions(Ref(k),2)^2;
end

% Solving the problem
PosNx=A\b;

%Computing the error
ErrNx = sqrt((PosNx(1)-positions(Nx,1))^2+(PosNx(2)-...

```

```

    positions(Nx,2))^2);

%Graphical output
if G
    scatter(positions(:,1),positions(:,2));
    xlabel('X [m]');
    ylabel('Y [m]');
    box on;
    hold on;
    scatter(PosNx(1), PosNx(2), 200, 'filled', 'k','p');
    scatter(positions(Nx,1),positions(Nx,2),200,...
        'filled','^');
    for i=1:k
        scatter(positions(Ref(i),1),positions(Ref(i),2),...
            'filled','r','s');
    end
    hold off;
end
end

```

A.2.2 *posisjonering.m*

```

%The function simulates the ranging procedure between the reference nodes
%and the target node. Parameters set in this file apply for
%'Posisjonering_hovedfil.m' also.
%The file sets up and simulates the communication between the reference
%nodes and the target node (transmitter/receiver communication) while
%taking into account time delays and channel models. Noise is also added at
%the receiver in order to make the simulations more realistic.
%
%Function input: 'distanse' (The real ranges estimated in
% Posisjonering_hovedfil.m)
%Function output: 'estimert_avstand' (estimated ranges/distances after the
% signal has been subjected to delay and
% the channel model)
%
%
function [estimert_avstand] = posisjonering(distanse)
%%%%%%%%%%%%%%%%%%%%%%%%%%%%%%%%%%%%%%%%%%%%%%%%%%%%%%%%%%%%%%%%%%%%%%%%

```

```

%parameters
%%%%%%%%%%%%%%%%%%%%%%%%%%%%%%%%%%%%%%%%%%%%%%%%%%%%%%%%%%%%%%%%%%%%%%%%
%distanse=[2]
rand('state',sum(100*clock))

Pow=-10; %The power available
fc =44e9; %Sampling frequency of the output signal
dPPM = 0.5e-9;%value of the PPM shift
dt=1/fc;
delta=100e-9; %Delay time before response

%%%%%%%%%%%%%%%%%%%%%%%%%%%%%%%%%%%%%%%%%%%%%%%%%%%%%%%%%%%%%%%%%%%%%%%%
%NODE INFO [Node(1),Node(2),Node(n)...Node(n+1)] %
%%%%%%%%%%%%%%%%%%%%%%%%%%%%%%%%%%%%%%%%%%%%%%%%%%%%%%%%%%%%%%%%%%%%%%%%
for k=1:length(distanse)

%distanse=[4.234 4.234];

LOSNLOS = [1 1 1 1 1 1 1 1 1]; %1=LOS(Line of sight) 0=NLOS(Non Line Of Sight)
Ns=[12];%The nubner of pulses to be produced for each bit
Ts =[9e-9];%Pulse repetition period, determines the position in
%time of each pulse
sendebits=cp0201_bits(1);%generates a random bit stream

%%%%%%%%%%%%%%%%%%%%%%%%%%%%%%%%%%%%%%%%%%%%%%%%%%%%%%%%%%%%%%%%%%%%%%%%
%Transmitter
%%%%%%%%%%%%%%%%%%%%%%%%%%%%%%%%%%%%%%%%%%%%%%%%%%%%%%%%%%%%%%%%%%%%%%%%
for n=1:1;
bits= sendebits;
[bits,THcodes(n,:),Stxtot,Referanse]=...
cp0201_transmitter_2PPM_TH_2(bits,dPPM,fc,Ns,Ts,Pow);
rate=1/(Ts(n)*Ns(n));
disp(['Node ' num2str(n) ': ' num2str(rate) ' Bit/sec'])
end

%%%%%%%%%%%%%%%%%%%%%%%%%%%%%%%%%%%%%%%%%%%%%%%%%%%%%%%%%%%%%%%%%%%%%%%%
%Generates the delayed signal
%%%%%%%%%%%%%%%%%%%%%%%%%%%%%%%%%%%%%%%%%%%%%%%%%%%%%%%%%%%%%%%%%%%%%%%%
%Stx_delay(n,:)=delayed signal
%%%%%%%%%%%%%%%%%%%%%%%%%%%%%%%%%%%%%%%%%%%%%%%%%%%%%%%%%%%%%%%%%%%%%%%%

```

```

for n=1:2
delay=distanse(k)/299792458; %time delay of the signal
                                %based on the speed of light

g=length(Stxtot);
xg=3*g;
pilot(n,:)=zeros(1,xg);
pilot(n,1:g)=Stxtot;
[Stx_delay(n,:)] = cp0804_signalshift(pilot(n,:),fc,delay);
end

%%%%%%%%%%%%%%%%%%%%%%%%%%%%%%%%%%%%%%%%%%%%%%%%%%%%%%%%%%%%%%%%%%%%%%%%
%Generates channel model
%%%%%%%%%%%%%%%%%%%%%%%%%%%%%%%%%%%%%%%%%%%%%%%%%%%%%%%%%%%%%%%%%%%%%%%%
%hf{n}=discrete channel model
%SRXHF{n}=attenuated and delayed signal at the receiver
%tstemp(n)
%%%%%%%%%%%%%%%%%%%%%%%%%%%%%%%%%%%%%%%%%%%%%%%%%%%%%%%%%%%%%%%%%%%%%%%%
disp('- Channel model for the different nodes based on distance and LOS/NLOS!')
clear n;
for n=1:2;
%disp('- Wait.....')
antpulser=Ns*length(sendebits);
[hf{n}, tstemp(n), SRXHF{n}] = kanalmodell2(distanse(k), LOSNLOS(k), ...
antpulser, fc, Stx_delay(n,:));
end
%%%%%%%%%%%%%%%%%%%%%%%%%%%%%%%%%%%%%%%%%%%%%%%%%%%%%%%%%%%%%%%%%%%%%%%%

%%%%%%%%%%%%%%%%%%%%%%%%%%%%%%%%%%%%%%%%%%%%%%%%%%%%%%%%%%%%%%%%%%%%%%%%
%Generates correlator mask for rake receiver
%%%%%%%%%%%%%%%%%%%%%%%%%%%%%%%%%%%%%%%%%%%%%%%%%%%%%%%%%%%%%%%%%%%%%%%%
for n=1:2;
[G,T,NF,Arake{n},Srake{n},Prake{n}] = cp0803_rakeselector(hf{n}, ...
fc,tstemp(n),5,5);

tempconv=conv(Srake{n},pilot(n,:));
pilot_Srake(n,:)=tempconv(1:length(pilot(n,:)));
clear tempconv;
end

%%%%%%%%%%%%%%%%%%%%%%%%%%%%%%%%%%%%%%%%%%%%%%%%%%%%%%%%%%%%%%%%%%%%%%%%

```

```

%Detection and distance estimation at the receiver
%%%%%%%%%%%%%%%%%%%%%%%%%%%%%%%%%%%%%%%%%%%%%%%%%%%%%%%%%%%%%%%%%%%%%%%%
for n=1:2;
stoy=cp0801_Gnoise_mod(fc,SRXHF{n}); %Thermal noise at the receiver.
                                %The function is cp0801_Gnoise2.m modified

Rx_delay_stoy(n,:)=sumarray(SRXHF{n},stoy); %received signal
                                %at the receiver with noise included

[Korrelert_signal_kanal(n,:)] = cp0804_corrbyn(Rx_delay_stoy(n,:), ...
pilot_Srake(n,:),fc); %Correlation between the signal at the
                    %receiver input(the delayed noise-affected signal)
                    % and the Srake receiver.

[peak,index]=max(Korrelert_signal_kanal(n,:));
estimated_delay1(n)=index*dt %estimated delay for received signal at
                            %the point where the signal is at its strongest,
                            %in order to get a best possible reading.

%[peak,index]=max(Korrelert_signal(n,:));
%estimated_delay2(n)=index*dt %estimert forsinkelse for test signal

end

%%%%%%%%%%%%%%%%%%%%%%%%%%%%%%%%%%%%%%%%%%%%%%%%%%%%%%%%%%%%%%%%%%%%%%%%Ranging procedure according to the theory%%%%%%%%%%%%%%%%%%%%%%%%%%%%%%%%%%%%%%%%%%%%%%%%%%%%%%%%%%%%%%%%%%%%%%%%
t0=1;
t1=t0+estimated_delay1(1)+estimated_delay1(2)+delta %the time when the
%reference node receives the response package

estimert_forsinkelse(k)=(t1-t0-delta)/2
estimert_avstand(k)=estimert_forsinkelse(k)*299792458 %calculating the
%distance d between two nodes by multiplying
%the estimated delay with the speed of light.

end

```

A.2.3 *kanalmodell2.m*

```
%%%%%%%%%%%%%%%%%%%%%%%%%%%%%%%%%%%%%%%%%%%%%%%%%%%%%%%%%%%%%%%%%%%%%%%%
%                               Channel Model
%%%%%%%%%%%%%%%%%%%%%%%%%%%%%%%%%%%%%%%%%%%%%%%%%%%%%%%%%%%%%%%%%%%%%%%%
%This function simulates the channel model and the effects it has on
%the transmitted signal. The simulation is done according to the
%statistical model proposed by IEEE 802.15.SG3a. The channel impulse
%response is generated accordingly and the effects of path loss are also
%taken into account. Calculations are made to consider four different
%scenarios. These are LOS/NLOS for distances d<=4 meters and d>4 meters.
%The parameters are all set according to the assumptions proposed by [1]
%%%%%%%%%%%%%%%%%%%%%%%%%%%%%%%%%%%%%%%%%%%%%%%%%%%%%%%%%%%%%%%%%%%%%%%%

function [hf, ts2, SRX2] = kanalmodell(d, type, antpulser, fc, Stx)
%%%%%%%%%%%%%%%%%%%%%%%%%%%%%%%%%%%%%%%%%%%%%%%%%%%%%%%%%%%%%%%%%%%%%%%%
%d: The distance between transmitter and receiver
%A0: The referance attenuation
%type: 1=LOS(Line of sight) 0=NLOS(Non Line Of Sight)
%antpulser: Number of pulses
%exno: The ratio between the received energy within
%       %a single pulse and the noise level
%stx: The signal from the transmitter.
%hf: Discrete channel impulse response
%ts2= The time resolution in seconds
%SRX2: The received signal after transmission over the channel
%G: G=1 plots the channel model G=0 no plot.
%%%%%%%%%%%%%%%%%%%%%%%%%%%%%%%%%%%%%%%%%%%%%%%%%%%%%%%%%%%%%%%%%%%%%%%%
G=0;

%%%%%%%%%%%%%%%%%%%%%%%%%%%%%%%%%%%%%%%%%%%%%%%%%%%%%%%%%%%%%%%%%%%%%%%%
%Calculates the channel model based on LOS/NLOS and distance
%%%%%%%%%%%%%%%%%%%%%%%%%%%%%%%%%%%%%%%%%%%%%%%%%%%%%%%%%%%%%%%%%%%%%%%%&&&

if type==0 & d<=4
%NLOS 0-4 meters
```

```

%%%%%%%%%%%%%%%%%%%%%%%%%%%%%%%%%%%%%%%%%%%%%%%%%%%%%%%%%%%%%%%%%%%%%%%%
%Finds the attenuation coefficient based on the distance d
%%%%%%%%%%%%%%%%%%%%%%%%%%%%%%%%%%%%%%%%%%%%%%%%%%%%%%%%%%%%%%%%%%%%%%%%
tx=1;
A0=51;
c0=10^(-A0/20);
gamma=3.5;
[rx,attn]=cp0801_pathloss(tx,c0,d,gamma);
%%%%%%%%%%%%%%%%%%%%%%%%%%%%%%%%%%%%%%%%%%%%%%%%%%%%%%%%%%%%%%%%%%%%%%%%
%Generates the channel impulse response
%%%%%%%%%%%%%%%%%%%%%%%%%%%%%%%%%%%%%%%%%%%%%%%%%%%%%%%%%%%%%%%%%%%%%%%%
TMG=attn^2;%Average total multipath gain at distance d
[h0,hf,OT,ts,X] = cp0802_IEEEuwbNLOS4(fc,TMG,G);
ts2=ts;
end

```

```

if type==0 & d>4
%NLOS 4-10 meters
%%%%%%%%%%%%%%%%%%%%%%%%%%%%%%%%%%%%%%%%%%%%%%%%%%%%%%%%%%%%%%%%%%%%%%%%
%Finds the attenuation coefficient based on the distance d
%%%%%%%%%%%%%%%%%%%%%%%%%%%%%%%%%%%%%%%%%%%%%%%%%%%%%%%%%%%%%%%%%%%%%%%%
tx=1;
A0=51;
c0=10^(-A0/20);
gamma=3.5;
[rx,attn]=cp0801_pathloss(tx,c0,d,gamma);
%%%%%%%%%%%%%%%%%%%%%%%%%%%%%%%%%%%%%%%%%%%%%%%%%%%%%%%%%%%%%%%%%%%%%%%%
%Generates the channel impulse response
%%%%%%%%%%%%%%%%%%%%%%%%%%%%%%%%%%%%%%%%%%%%%%%%%%%%%%%%%%%%%%%%%%%%%%%%
TMG=attn^2;
[h0,hf,OT,ts,X] = cp0802_IEEEuwbNLOS10(fc,TMG,G);
ts2=ts;
end

```

```

if type==1 & d<=4
%LOS 0-4 meters
%%%%%%%%%%%%%%%%%%%%%%%%%%%%%%%%%%%%%%%%%%%%%%%%%%%%%%%%%%%%%%%%%%%%%%%%
%Finds the attenuation coefficient based on the distance d
%%%%%%%%%%%%%%%%%%%%%%%%%%%%%%%%%%%%%%%%%%%%%%%%%%%%%%%%%%%%%%%%%%%%%%%%
tx=1;

```

```

A0=47;
c0=10^(-A0/20);
gamma=1.7;
[rx,attn]=cp0801_pathloss(tx,c0,d,gamma);
%%%%%%%%%%%%%%%%%%%%%%%%%%%%%%%%%%%%%%%%%%%%%%%%%%%%%%%%%%%%%%%%%%%%%%%%
%Generates the channel impulse response
%%%%%%%%%%%%%%%%%%%%%%%%%%%%%%%%%%%%%%%%%%%%%%%%%%%%%%%%%%%%%%%%%%%%%%%%
TMG=attn^2;
[h0,hf,OT,ts,X] = cp0802_IEEEuwbLOS4(fc,TMG,G);
ts2=ts;
end

if type==1 & d>4
%LOS 4-15 meters
%%%%%%%%%%%%%%%%%%%%%%%%%%%%%%%%%%%%%%%%%%%%%%%%%%%%%%%%%%%%%%%%%%%%%%%%
%Finds the attenuation coefficient based on the distance d
%%%%%%%%%%%%%%%%%%%%%%%%%%%%%%%%%%%%%%%%%%%%%%%%%%%%%%%%%%%%%%%%%%%%%%%%
tx=1;
A0=47;
c0=10^(-A0/20);
gamma=1.7;
[rx,attn]=cp0801_pathloss(tx,c0,d,gamma);
%%%%%%%%%%%%%%%%%%%%%%%%%%%%%%%%%%%%%%%%%%%%%%%%%%%%%%%%%%%%%%%%%%%%%%%%
%Generates the channel impulse response
%%%%%%%%%%%%%%%%%%%%%%%%%%%%%%%%%%%%%%%%%%%%%%%%%%%%%%%%%%%%%%%%%%%%%%%%
TMG=attn^2;
[h0,hf,OT,ts,X] = cp0802_IEEEuwbLOS10(fc,TMG,G);
ts2=ts;
end
%%%%%%%%%%%%%%%%%%%%%%%%%%%%%%%%%%%%%%%%%%%%%%%%%%%%%%%%%%%%%%%%%%%%%%%%

SRX = conv(Stx,hf);
SRX2 = SRX(1:length(Stx)); %The signal after transmission over
the channel

```

A.2.4 *cp0802_IEEEubLOS4.m*

```
%This function is almost unchanged from the original cp0802_IEEEuwb.m
%programmed by Guerino Giancola. The author of the report has added
%the parameter G as to prevent the graphic display.
%Parameters OT, ts, LAMBDA, lambda, Gamma and gamma have also been
%changed as to fit the LOS profile according to the proposals in [2].
%Files cp0802_IEEEuwbLOS10.m, cp0802_IEEEuwbNLOS4.m, and
%cp0802_IEEEuwbNLOS10.m have been edited in the same way and will
%not be listed in the appendix.
%%%%%%%%%%%%%%%%%%%%%%%%%%%%%%%%%%%%%%%%%%%%%%%%%%%%%%%%%%%%%%%%%%%%%%%%
% FUNCTION 8.8 : "cp0802_IEEEuwb"
%
% Generates the channel impulse response for a multipath
% channel according to the statistical model proposed by
% the IEEE 802.15.SG3a.
%
% 'fc' is the sampling frequency
% 'TMG' is the total multipath gain
%
% The function returns:
% 1) the channel impulse response 'h0'
% 2) the equivalent discrete-time impulse response 'hf'
% 3) the value of the Observation Time 'OT'
% 4) the value of the resolution time 'ts'
% 5) the value of the total multipath gain 'X'
%
% Programmed by Guerino Giancola
%

function [h0,hf,OT,ts,X] = cp0802_IEEEuwbLOS4(fc,TMG,G);

% -----
% Step Zero - Input parameters
% -----

OT = 200e-9;           % Observation Time [s]
ts = 1e-9;            % time resolution [s]
```

```

                                % i.e. the 'bin' duration

LAMBDA = 0.0233*1e9;           % Cluster Arrival Rate (1/s)
lambda = 2.5e9;                % Ray Arrival Rate (1/s)
GAMMA = 7.1e-9;                % Cluster decay factor
gamma = 4.3e-9;                % Ray decay factor
sigma1 = 10^(3.3941/10);       % Stdev of the cluster fading
sigma2 = 10^(3.3941/10);       % Stdev of the ray fading
sigmax = 10^(3/10);            % Stdev of lognormal shadowing

% ray decay threshold
rdt = 0.001;
% rays are neglected when exp(-t/gamma)<rdt

% peak treshold [dB]
PT = 50;
% rays are considered if their amplitude is
% within the -PT range with respect to the peak

% -----
% Step One - Cluster characterization
% -----

dt = 1 / fc;                    % sampling time

T = 1 / LAMBDA;                 % Average cluster inter-arrival time
                                % [s]
t = 1 / lambda;                 % Average ray inter-arrival time [s]

i = 1;
CAT(i)=0;                       % First Cluster Arrival Time
next = 0;
while next < OT
    i = i + 1;
    next = next + expinv(rand,T);
    if next < OT
        CAT(i)= next;
    end
end % while remaining > 0

```

```

% -----
% Step Two - Path characterization
% -----

NC = length(CAT); % Number of observed clusters
logvar = (1/20)*((sigma1^2)+(sigma2^2))*log(10);
omega = 1;
pc = 0; % path-counter

for i = 1 : NC

    pc = pc + 1;
    CT = CAT(i); % cluster time

    HT(pc) = CT;

    next = 0;
    mx = 10*log(omega)-(10*CT/GAMMA);
    mu = (mx/log(10))-logvar;
    a = 10^((mu+(sigma1*randn)+(sigma2*randn))/20);

    HA(pc) = ((rand>0.5)*2-1).*a;

    ccoeff = sigma1*randn; % fast fading on the cluster

    while exp(-next/gamma)>rdt

        pc = pc + 1;
        next = next + expinv(rand,t);
        HT(pc) = CT + next;
        mx = 10*log(omega)-(10*CT/GAMMA)-(10*next/GAMMA);
        mu = (mx/log(10))-logvar;
        a = 10^((mu+ccoeff+(sigma2*randn))/20);
        HA(pc) = ((rand>0.5)*2-1).*a;

    end

end % for i = 1 : NC

% Weak peak filtering

```

```

peak = abs(max(HA));
limit = peak/10^(PT/10);
HA = HA .* (abs(HA)>(limit.*ones(1,length(HA))));

for i = 1 : pc
    itk = floor(HT(i)/dt);
    h(itk+1) = HA(i);
end

% -----
% Step Three - Discrete time impulse response
% -----

N = floor(ts/dt);
L = N*ceil(length(h)/N);
h0 = zeros(1,L);
hf = h0;
h0(1:length(h)) = h;
for i = 1 : (length(h0)/N)
    tmp = 0;
    for j = 1 : N
        tmp = tmp + h0(j+(i-1)*N);
    end
    hf(1+(i-1)*N) = tmp;
end

% Energy normalization
E_tot=sum(h.^2);
h0 = h0 / sqrt(E_tot);
E_tot=sum(hf.^2);
hf = hf / sqrt(E_tot);

% Log-normal shadowing
mux = ((10*log(TMG))/log(10)) - (((sigmax^2)*log(10))/20);

X = 10^((mux+(sigmax*randn))/20);

h0 = X.*h0;
hf = X.*hf;

```

```

% -----
% Step Four - Graphical Output
% -----

if G

    Tmax = dt*length(h0);
    time = (0:dt:Tmax-dt);

    figure(1)
    S1=stem(time,h0);
    AX=gca;
    set(AX,'FontSize',14);
    T=title('Channel Impulse Response');
    set(T,'FontSize',14);
    x=xlabel('Time [s]');
    set(x,'FontSize',14);
    y=ylabel('Amplitude Gain');
    set(y,'FontSize',14);
    figure(2)
    S2=stairs(time,hf);
    AX=gca;
    set(AX,'FontSize',14);
    T=title('Discrete Time Impulse Response');
    set(T,'FontSize',14);
    x=xlabel('Time [s]');
    set(x,'FontSize',14);
    y=ylabel('Amplitude Gain');
    set(y,'FontSize',14);

end

```

A.2.5 *cp0801_Gnoise_mod.m*

```

%%%%%%%%%%%%%%%%%%%%%%%%%%%%%%%%%%%%%%%%%%%%%%%%%%%%%%%%%%%%%%%%%%%%%%%%
%This function simulates the noise that is added to the
%signal at the receiver. The noise is generated by first

```

```

%generating a signal that is then attenuated by information
%by factors given in [2]. The value of exno for a certain
%distance d is also gathered from the same source. The
%function is based on "cp0801_Gnoise2" programmed by
%Guerino Giancola in [1].
%%%%%%%%%%%%%%%%%%%%%%%%%%%%%%%%%%%%%%%%%%%%%%%%%%%%%%%%%%%%%%%%%%%%%%%%
%%
% Introduces additive white Gaussian noise over signal
% 'input'.
% Vector 'exno' contains the target values of Ex/No (in dB)
% 'numpulses' is the number of pulses composing the input
% signal
%
% Multiple output signals are generated, one signal for
% each target value of Ex/No. The array 'output' contains
% all the signals (input+AWGN), one signal per row.
% The array 'noise' contains the different realization of
% the Gaussian noise, one realization per each row.
%
%
%

function [noise] = ...
    cp0801_Gnoise_mod(fc,lengdeoutput)

% -----
% Step One - Introduction of AWGN
% -----

fc = 5e9;
dPPM = 0.5e-9;

bits=cp0201_bits(200);
[bits,THcoda,Stxta,Refa]=cp0201_transmitter_2PPM_TH_3(bits, ...
0.5e-9,fc,1,62e-9,-2.5);

d=6;
tx=1;
A0=47;
c0=10^(-A0/20);
gamma=1.7;

```

```

[rx,attn]=cp0801_pathloss(tx,c0,d,gamma);
input=Stxta.*attn;
exno=14.9;

numpulses=length(bits);
%%%%%%%%%%%%%%%%%%%%%%%%%%%%%%%%%%%%%%%%%%%%%%%%%%%%%%%%%%%%%%%%%%%%%%%%

Ex = (1/numpulses)*sum(input.^2); % measured energy per
                                   % pulse
ExNo = 10.^(exno./10);           % Ex/No in linear units
No = Ex ./ ExNo;                 % Unilateral spectral
                                   % density
nstdv = sqrt(No./2);             % Standard deviation for
                                   % the noise

for j = 1 : length(ExNo)

    noise(j,:) = nstdv(j) .* randn(1,length(lengdeoutput));

end

```

A.2.6 *cp0201_transmitter_2PPM_TH_2*

```

%This file is entirely programmed by Guerino Giancola.
%The author has only adapted it so that some variables
%are received as an input instead of being predefined.
%Also, the random bit sequence is generated in posisjoning.m
%as well, and is thus received as an input.
%%%%%%%%%%%%%%%%%%%%%%%%%%%%%%%%%%%%%%%%%%%%%%%%%%%%%%%%%%%%%%%%%%%%%%%%
%
%
% FUNCTION 2.6 : "cp0201_transmitter_2PPM_TH"
%
% Simulation of a UWB transmitter implementing 2PPM with TH

```

```

%
% Transmitted Power is fixed to 'Pow'
% The signal is sampled with frequency 'fc'
% 'numbits' is the number of bits generated by the source
% 'Ns' pulses are generated for each bit, and these pulses
% are spaced in time by an average pulse repetition period
% 'Ts'
% The TH code has periodicity 'Np', and cardinality 'Nh'
% The chip time has time duration 'Tc'
% Each pulse has time duration 'Tm' and shaping factor
% 'tau'
% The PPM introduces a time shift of 'dPPM'
%
% The function returns:
% 1) the generated stream of bits ('bits')
% 2) the generated TH code ('THcode')
% 3) the generated signal ('Stx')
% 4) a reference signal without data modulation ('ref')
%
% Programmed by Guerino Giancola
%

function [bits,THcode,Stx,ref]=cp0201_transmitter_2PPM_TH(bits, ...
dPPM,fc,Ns,Ts,Pow)

% -----
% Step Zero - Input parameters
% -----

%Pow = -20;          % average transmitted power (dBm)

%fc = 50e9;         % sampling frequency

numbits = length(bits);    % number of bits generated by the source

%Ts = 3e-9;         % frame time, i.e., average pulse
                    % repetition period [s]
% Ns = 1            ;number of pulses per bit

Tc = 1e-9;         % chip time [s]
Nh = 9;           % cardinality of the TH code

```

```

Np = 5;          % periodicity of the TH code

Tm = 0.5e-9;    % pulse duration [s]
%Tm = 800e-12;
tau = 0.25e-9;  % shaping factor for the pulse [s]
%dPPM = 0.5e-9; % time shift introduced by the PPM [s]

G = 0;
% G=0 -> no graphical output
% G=1 -> graphical output

% -----
% Step One - Simulating transmission chain
% -----

% repetition coder
repbits = cp0201_repcode(bits,Ns);

% TH code
THcode = cp0201_TH(Nh,Np);

% PPM + TH
[PPMTHseq,THseq] = ...
    cp0201_2PPM_TH(repbits,fc,Tc,Ts,dPPM,THcode);

% shaping filter
power = (10^(Pow/10))/1000;    % average transmitted power
                                % (watt)
Ex = power * Ts;              % energy per pulse
w0 = cp0201_waveform(fc,Tm,tau);% energy normalized pulse
                                % waveform
wtx = w0 .* sqrt(Ex);         % pulse waveform
Sa = conv(PPMTHseq,wtx);     % output of the filter
                                % (with modulation)
Sb = conv(THseq,wtx);        % output of the filter
                                % (without modulation)

% Output generation

```

```

L = (floor(Ts*fc))*Ns*numbits;
Stx = Sa(1:L);
ref = Sb(1:L);

% -----
% Step Two - Graphical output
% -----

if G

F = figure(1);
set(F,'Position',[32 223 951 420]);

tmax = numbits*Ns*Ts;
time = linspace(0,tmax,length(Stx));
P = plot(time,Stx);
set(P,'LineWidth',[2]);
ylo=-1.5*abs(min(wtx));
yhi=1.5*max(wtx);
axis([0 tmax ylo yhi]);
AX=gca;
set(AX,'FontSize',12);
X=xlabel('Time [s]');
set(X,'FontSize',14);
Y=ylabel('Amplitude [V]');
set(Y,'FontSize',14);
for j = 1 : numbits
    tj = (j-1)*Ns*Ts;
    L1=line([tj tj],[ylo yhi]);
    set(L1,'Color',[0 0 0],'LineStyle', ...
        '--','LineWidth',[2]);
    for k = 0 : Ns-1
        if k > 0
            tn = tj + k*Nh*Tc;
            L2=line([tn tn],[ylo yhi]);
            set(L2,'Color',[0.5 0.5 0.5],'LineStyle', ...
                '-.','LineWidth',[2]);
        end
    for q = 1 : Nh-1
        th = tj + k*Nh*Tc + q*Tc;

```

```
        L3=line([th th],[0.8*ylow 0.8*yhigh]);
        set(L3,'Color',[0 0 0],'LineStyle', ...
            ':' , 'LineWidth',[1]);
    end
end
end

end % end of graphical output
```

A.2.7 *cp0201_transmitter_2PPM_TH_3*

The same changes have been performed as described for *cp0201_transmitter_2PPM_TH_3*.